ESA Lakes_CCI+ - Phase 2
Lake Storage Change option

D1.1 State of the art

D1.2 User requirement

ESA contract : 4000125030/18/I-NB – Lakes_cci
Doc Ref. CCI-Lakes2-0010-TN

Version 1.3 – 11/04/2023

11 rue Hermès, Parc Technologique du Canal — 31520 Ramonville Saint-Agne, France
Tel +33 (0)5 61 39 47 00 Fax +33(0)5 61 75 10 14
www.cls.fr

CHRONOLOGY ISSUES

Issue	Date	Object	Written by
1.0	10/02/23	Initial version	C.Fatras
1.1	27/03/23	Internal review	C.Fatras
1.3	11/04/23	New version that includes ESA comments	C.Fatras

Checked by	Stefan Simis – PML J-F Cretaux - LEGOS	S Simis 24 Apr 2023
Approved by	Alice Andral - CLS	 24 avr. 2023
Authorized by	Clément Albergel - ESA	Albergel C 24 avr. 2023

DISTRIBUTION

Company	Names	Email
ESA	Clément Albergel	clement.albergel@esa.int
BC	Carsten Brockman	carsten.brockmann@brockmann-consult.de
BC	Kerstin Stelzer	kerstin.stelzer@brockmann-consult.de
CLS	Alice Andral	aandral@groupcls.com
CLS	Anna Mangilli	amangilli@groupcls.com
CLS	Beatriz Calmettes	bcalmettes@groupcls.com
CLS	Pierre Thibault	pthibaut@groupcls.com
CLS	Yann Bernard	ybernard@groupcls.com
CNR	Claudia Giardino	giardino.c@irea.cnr.it
CNR	Gary Free	free.g@irea.cnr.it
CNR	Mariano Bresciani	bresciani.m@irea.cnr.it
CNR	Monica Pinardi	pinardi.m@irea.cnr.it
CNR	Marina Amadori	amadori.m@irea.cnr.it
H2O Geo	Claude Duguay	claude.duguay@h2ogeomatics.com
H2O Geo	Yuhao Wu	mark.wu@h2ogeomatics.com
LEGOS	Jean-François Cretaux	Jean-Francois.Cretaux@legos.obs-mip.fr
PML	Stefan Simis	stsi@pml.ac.uk
PML	Xiaohan Liu	liux@pml.ac.uk
Sertit	Hervé Yésou	Herve.yesou@unistra.fr
Sertit	Jérôme Maxant	maxant@unistra.fr
Sertit	Rémi Braun	remi.braun@unistra.fr
UoR	Chris Merchant	c.j.merchant@reading.ac.uk
UoB	Iestyn Woolway	Iestyn.woolway@bangor.ac.uk
UoR	Laura Carrea	l.carrea@reading.ac.uk
UoS	Dalin Jiang	dalin.jiang@stir.ac.uk
UoS	Evangelos Spyrakos	evangelos.spyrakos@stir.ac.uk
UoS	Ian Jones	ian.jones@stir.ac.uk

LIST OF CONTENTS

1 Purpose of this document....6
2 State of the art of lake storage change retrieval....6
2.1 Lake storage change estimation....7
2.1.1 Power law and polynomial fitting for direct estimation of volumes....7
2.1.2 Global approach for water volume estimation without hypsometric curves....9
2.1.3 Estimation of LSC from a hypsometric curve....10
2.2 Hypsometric curve estimation....11
2.2.1 Hypsometry from geomorphic processes....11
2.2.2 Hypsometry from altimetry & surfaces....12
2.3 Water level estimation....14
2.3.1 Altimetry water height estimation....14
2.3.2 Water elevation from Digital Elevation Model....16
2.4 Water surface extent estimation....18
2.4.1 Dynamic approaches....18
2.4.2 Static data: the Global Surface Water dataset....23
2.5 Perspectives on Bathymetry estimation for lake volume estimation....23
3 User requirements....26
4 Benchmark activities....28
5 Study sites....29
Appendix A - Bibliography....31
Appendix B - GSW methodology to retrieve water extent....35

LIST OF TABLES AND FIGURES

Figure 1 – Pipeline proposed in the frame of the ESA CCI LSC option 6
Figure 2 – Comparison of the two storage curves of Fengman reservoir (Peng et al. 2006) 8
Figure 3 – Volume variation between water height H1 and H2 and corresponding areas A1 and A2 10
Figure 4 – Hypsometric curves classification (from Wilgoose & Hancock 1998) 12
Figure 5 – Principle of hypsometric curve (estimated in red) for lake studies 12
Figure 6 – Hypsometry polynomial of Lake Ayakkum (within the hypsometry equation, height is expressed in meters and area in km²) (from Crétaux et al., 2016) 13
Figure 7 – Original Strahler approach (left) and modified Strahler approach based on water levels and surface areas (right). (from Schwatke et al. 2020). 14
Figure 8 - Timeline for satellite altimeters. Dashed lines correspond to major orbit change. Blue lines correspond to altimeters used for continental hydrology purposes. 15
Figure 9 – Statistics on the DAHITI database of virtual stations, by continent and by types (as of March 2023) 16
Figure 10 - Shoreline of the Laaba basin for six different dates (from Amitrano et al. 2014) 17
Figure 11 - Band availability and lifespan of the main optical satellites. Landsat 7 experienced from 2003 a sensor incident that deteriorated strongly the data acquisition (dashed line). 19
Figure 12 – Lake Waduk Cirata (Indonesia), here depicted in false colours from Sentinel-2 with red areas corresponding to vegetation. It presents floating vegetation, houses and fishery ponds on its surface, that make it difficult to precisely determine the lake water surface. 20
Figure 13 - Principle of Otsu Sequencing on contours (from Donchyts et al., 2016) 21
Figure 14 - Global water data derived from the 8,756 Landsat ETM+ images in the GLS2000 dataset (from Feng et al., 2016) 22
Figure 15 - Location of the twenty study lakes around the world 29
Figure 16 - Test lakes and their description following the selection criteria 30
Figure 17 – Diagram of the expert system classifier (from Pekel et al., 2016) 35
Figure 18 – Example of water occurrence from the GSW Occurrence dataset, here in Cambodia. 36

Table 1 – Formulas for water volume variation estimation between two states 11
Table 2 - List of optical indexes used for water detection 19

REFERENCE DOCUMENTS

Reference	Name	Access
[R1] CCI-LAKES-0024-ATBD_v2.1	ATBD of Lake Water Extent ECV	https://climate.esa.int/en/projects/lakes/key-documents-lakes/
[R2] CCI_LAKES2-0005-URD	User requirement Document of Lakes_CCI project Phase 2	https://climate.esa.int/en/projects/lakes/key-documents-lakes/

1 Purpose of this document

The objective of this document is to review the different methodologies to retrieve lake storage change for lakes and reservoirs globally and with a temporal depth sufficient for climate studies and climate modelling. It will guide the benchmarking that will be done in the forthcoming step of this analysis. This report summarises also the user requirements for the lake storage change in relation to the state of the art.

2 State of the art of lake storage change retrieval

The following diagram depicts the different steps to estimate lake storage change of lakes and reservoirs. The first studies of lake storage change appeared in the end of the 1990s and begun with in-situ data of height and water surface areas and/or volume to retrieve water volume at local or regional scale. With the increasing volume of satellite data, research since focused on the production of height and water surface area information from remote sensing. This opened the way to the estimation of the Lake Storage Change (LSC), but also defined the requirements in terms of surface areas and height accuracy for the determination of a precise lake storage change estimation.

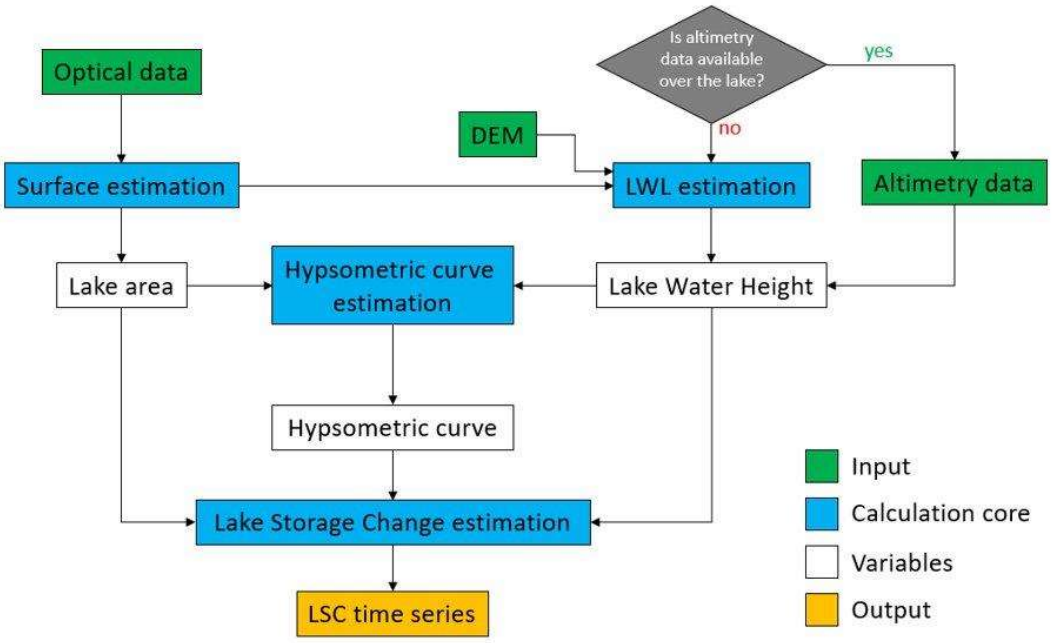

Figure 1 – Pipeline proposed in the frame of the ESA CCI LSC option

Each step of the diagram is described in the following section. Therefore, the first part explores the global water volume change estimation from power law and other polynomial calibration, fitting, or lake variation integration. Then, we focus on the hypsometric curve estimation, first from a geomorphological point of view, then from altimetry and surface areas applied to water volume estimation. The two next steps detail the different data that can be used for water level (i.e., altimetry and DEM) and water surface areas. And finally, we present the perspectives in retrieving the total water volume estimation and bathymetry.

2.1 Lake storage change estimation

Two fields off research are combined in this work: total volume estimation and lake storage change. The first focuses on the total water available in a water body, with uncertainties generally corresponding to lack of information on water depth. The second deals with lakes storage change, deduced from the relation between information of water level and surface extent. This relation is always positive, usually described by a power law or a polynomial approach. Nevertheless, total water volume cannot be deduced from these laws directly.

In this chapter, we will focus first on direct approaches to retrieve total volume of lake and reservoirs with power law and polynomial fitting, then, on approaches without hypsometric curves and finally, on approaches with hypsometric curve (as used by the CCI Lakes project to retrieve Lake Water Extent).

2.1.1 Power law and polynomial fitting for direct estimation of volumes

A relation between small reservoir surface areas with their corresponding capacity comes from Meigh 1995, in Botswana. Without remote sensing input and if the area *A* is constant for each considered reservoir, this is a direct attempt to relate the capacity of the reservoirs from the area following a power calibration law (of the type $V = a * A^b$, *V* being the volume, and *a* & *b* being scalar parameters).

This approach has been furthered in Liebe 2002 for 61 reservoirs in Ghana using optical remote sensing data. After assessing water surface area from remote sensing compared with in situ data, reservoir volume variation is derived from the water surface areas change in time. It is shown that the logarithms of surface area and volume are linearly correlated. Nevertheless, the height-volume relationships established are estimated from one surface area per reservoir only, and is an important source of errors for different water surfaces areas. This shows that 1) the absence of hypsometric consideration might lead to considerable uncertainty of estimates in volume estimation, 2) this work is applicable for similar areas in terms of geomorphologic properties, meaning that it is not valid for a global approach. Note that these results are slightly enhanced and improved in the following work exposed in Liebe et al. 2005.

With static water areas (i.e., that does not represent the potential water surface area change with time) from field and remote sensing images, Sawunyama et al. 2006 retrieved a linear relationship between the logarithms of water surface area and water capacity for approximately 1000 reservoirs in the Mzingwane catchment of Zimbabwe. This agrees, along with the results from Liebe et al 2002, 2005, with the existence of a common behaviour between reservoir capacity and surface area for catchments with similar geomorphological properties. As mentioned in the conclusion of Sawunyama et al. 2006, results worsen for very steep valleys, and a homogeneity in the geomorphologically coherent area is needed for the validity of these relationships (i.e., Head-Area-Volume, or H-A-V).

Once again in Ghana, Annor et al. 2009 focused on the delineation of small reservoirs using radar imagery in a semi-arid environment. Following the work initiated by Liebe 2002, they managed to produce volume estimates on 21 small reservoirs of the study area. They found that the values of the parameters *a* and *b* in the power law are surprisingly constant within geomorphologically similar areas; nevertheless, this assumption remains to be tested in other locations.

Vanthof & Kelly 2019 explored determining water storage in ungauged small reservoirs with the TanDEM-X DEM, along with multi-source satellite observations. They established for 72 reservoirs in the Gundar river basin (India) the Volume-Area relationship from waterless DEM (TanDEM-X) once again

through a power law. Then from time series of surface areas, they were able to produce volume variation time series. They also found that the values of *a* and *b* in the power law are surprisingly constant within the same catchment; they explained this stability of the two parameters by a high similarity of the whole area geomorphologically wise.

From these studies, if the power law represents a good option to represent the relation between the area and the volume at a catchment level from various reservoirs, this approach seems to have been applied only for reservoirs and not lakes. This encouraging approach will be tested during the benchmark phase. The precision of the water content of reservoirs at different levels has not been explored in detail, but the methodology will be tested for precise water volume estimation. The geomorphological approach and its coherence at a catchment level is an interesting characteristic that could be furthered on.

Following the use of remote sensing data, Peng et al. 2006 has shown potential to produce reservoir volume variation time series for the Fengman dam reservoir (Songhua Lake) in Northeastern China. They compared the results they produced with an in-situ water level – storage curve produced in 1956 during the building of this dam. They used order 4 polynomial fitting to estimate H-A and H-V curves from altimetry and Landsat imagery. Whilst a promising approach to estimate water storage variation, this is only tested in one lake in this one case, without justification of choosing a 4th order polynomial or discussing the (slight) difference from the 1956 curve and the 2006 curve from remote sensing data.

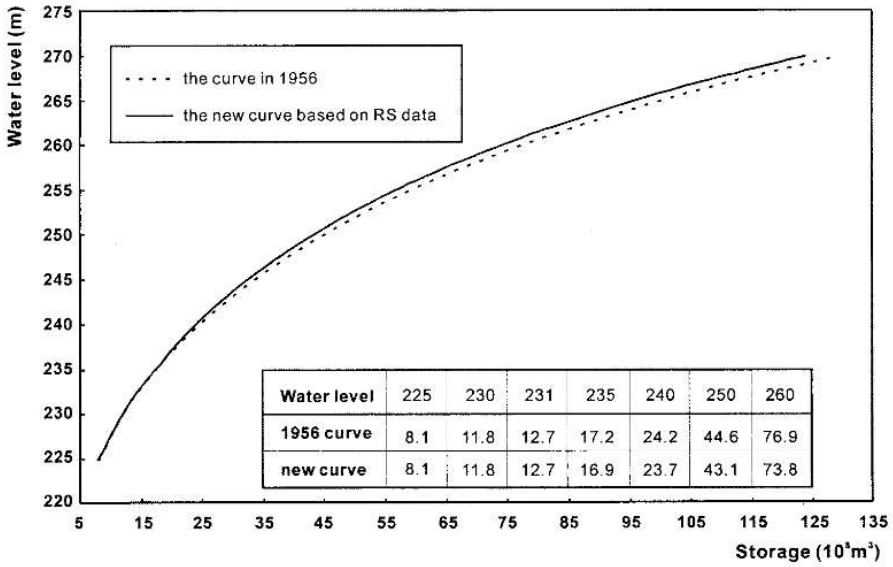

Water level	225	230	231	235	240	250	260
1956 curve	8.1	11.8	12.7	17.2	24.2	44.6	76.9
new curve	8.1	11.8	12.7	16.9	23.7	43.1	73.8

Figure 2 – Comparison of the two storage curves of Fengman reservoir (Peng et al. 2006)

Duan & Bastiaanssen (2013) link water surface areas from lakes and reservoirs to altimetry data products from existing databases, notably the Global Reservoir and Lake Monitoring (GRLM), River Lake Hydrology (RLH), Hydroweb, ICESat-GLAS level 2 Global Land Surface Altimetry data (ICESat-GLAS). They introduced the Water Volume Above the Lowest water Level (WVALL) concept, and tested it over three large lakes (Tana, Mead and IJssel). They link water height and areas for these three lakes with a 2nd order polynomial. Their validation procedure showed that estimated water volumes agreed well with in-situ measurements (R^2 from 0.95 to 0.99) and the root mean square error (RMSE) was within 4.6 to 13.1% of the mean volumes of in-situ measurements." Nevertheless, this relation in this particular paper has been tested only for very large lakes, with almost linear trends.

Table 1 - Symbolic representation of power laws for both volume and area estimations

	Power law	Polynomial
Volume	$V = cH^d$	$V = aH^4 + bH^3 + cH^2 + dH^1 + e$

Area	$A = aH^b$	$A = aH^4 + bH^3 + cH^2 + dH^1 + e$

With A being the water area, H the water height, V the water volume, and a, b, c, d and e empirical fitting coefficients.

⇨ As part of our planned benchmarking exercise, we will assess the accuracy of these power laws to relate area and volume with height on test lakes.

2.1.2 Global approach for water volume estimation without hypsometric curves

In the previous section, we presented research focusing on the estimation of reservoir volumes from power law and polynomial fitting linking water area and/or height to volume at a local or regional scale in some selected places. Here, we present methodologies using height and surface area to retrieve water volume without relying on hypsometric curves.

Messager et al 2016 proposed the first total water content estimation at a global scale. They used a model linking the surrounding topography of lakes and reservoirs to their estimated bathymetry. The lakes are defined from static databases, like the SRTM water bodies (accessible here) or CanVec dataset for Canada (accessible here). They applied a group-specific multiple regression using surface area together with terrain and lake shape variables as predictors. They created a bathymetry estimate for 1.42 million lakes and reservoirs worldwide. However, the resulting estimates of lake water volumes are static in time. The validation on a short dataset cannot ensure the validity of the estimated lakes and reservoirs depths estimations on the whole database, so these estimates are to be taken cautiously.

To apprehend temporal variation of water volume, Cooley et al. 2021 linked information from static surface areas to water height variations from ICEsat-2. Yet, the use of Icesat2 with a low repeatability involves some imprecisions. With ICEsat-2, they considered 227,386 water bodies with at least two water level information from October 2018 to July 2020. The water surface area in this study was considered static, using the surface area corresponding to occurrences higher than 75% in the Global Surface Water Occurrence dataset (Pekel et al. 2016) and eroded by 3 pixels. They also excluded rivers from the analysis by flagging water bodies with an extent inferior to 5% compared to their bounding box area.) For the LSC estimation we want to propose, it seems that long time series of water total volume cannot be estimated from only two water height measurements with sufficient accuracy, and the surface area variation may not be properly captured this way. Nevertheless, this study emphasizes that the uncertainty due to the use of static water areas is minor for low-varying water bodies (at least).

Khazaei et al 2022 propose and enhancement of the HydroLAKES database, the main difference being that this work adds bathymetric information and not only volumetric changes with time. The new database is called GLOBathy. It uses a GIS-based framework to generate bathymetric maps based on the waterbody maximum depth estimates and HydroLAKES geometric and geophysical attributes of the waterbodies. The maximum depth estimates are validated at 1,503 waterbodies, making use of several observed data sources. They also provide estimates for H-A-V relationships of the HydroLAKES waterbodies, driven from the bathymetric maps of the GLOBathy dataset. The H-A-V here are expressed as power laws. However, even if the results show satisfactory estimations, for natural lakes the maximum depth may not drive the behavior of the whole lake's bathymetry and might impede a confident use of the dataset. For this Lake Storage Change estimation activity, we will not consider this approach as we want a robust methodology for both lakes and reservoirs, and that without any doubt of introducing an error through a wrong bathymetry for the estimation of volume change.

Hou et al. 2022 also propose a geo-statistical method. They used high-resolution Landsat and Sentinel-2 optical remote sensing and ICESat-2 laser altimetry in addition to radar altimetry from the Topex/Poseidon, Jason-1, -2 and -3, and Sentinel-3 instruments. Past time series (1984-2020) of relative or absolute water surface extents for more than 170,000 lakes globally with a surface area of at least 1 km² were retrieved. Within these, they were able to develop an automated workflow for near real-time global lake monitoring of more than 27,000 lakes for 2020 onwards. Lake water volumes were estimated by the bias-corrected predicted water depths multiplied by water extents. Ultimately, they produced monthly water storage dynamics from 1984-2020 for 170,611 lakes globally. They also estimated relative lake storage dynamics from 2018 onwards for 23,419 lakes using ICESat-2 and Landsat, and from 1993 onwards for 148 lakes using G-REALM and Landsat. Their product comprises both relative and absolute volume estimates for all HydoLAKES delineated lakes larger than 1 km². They demonstrated that the geo-statistical HydroLAKES bathymetry estimation approach produced slightly better results than the GLOBathy method. Validation results showed an average *R* of 0.78 and a SMAPE of 52.5% between estimated and reported volumes for 238 lakes in USA and Australia. This result may yet be tempered by the difference in number of validation lakes and approaches between the data used in Messager et al. 2016 (12,150) and in Hou et al. 2022 (238). Therefore, for test lakes that are in the US of in Australia, we will compare the results with this study.

⇨ The use of geomorphological data along with remote sensing information for water height and water surface areas seems to provide satisfactory estimates of water volume at a global scale, which continue to improve. The approach by Hou et al., 2022 will be tested in US and Australian lakes included in our initial selection of 20 lakes.

2.1.3 Estimation of LSC from a hypsometric curve

Previously, power laws or cylindrical approximations directly linked the water height H to the total water content V from a power law. For more complex areas, this height's variation has an impact on area and hence volume, that can be expressed through a hypsometric curve. The definition and estimation of this curve are explored in the next section 2.2.

Here, the objective is to list the main methodologies to derive the volume variation (ΔV) from the related height or surface extent variation (respectively ΔH and ΔA). This is done using a power law as mentioned previously, or by using the hypsometric curve between two known states.

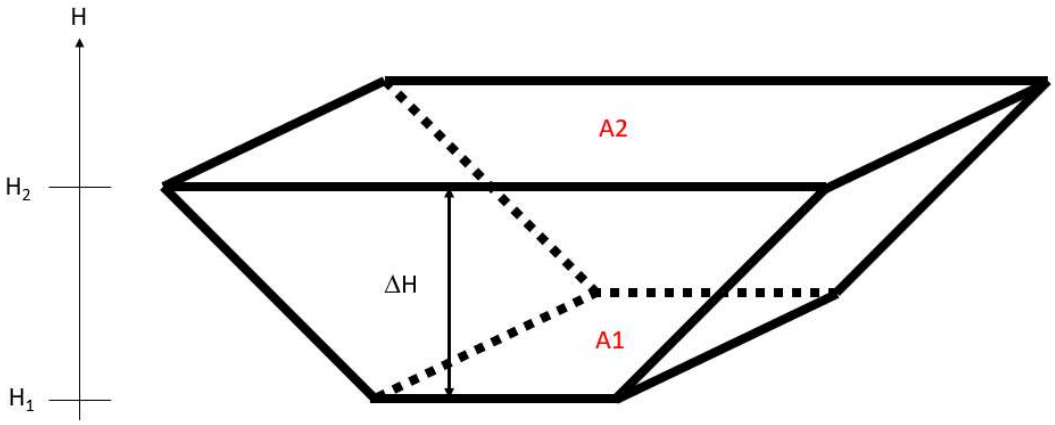

Figure 3 – Volume variation between water height H1 and H2 and corresponding areas A1 and A2

The studies explored to this purpose showed five different ways of estimating the water volume variation between two lake states. They are listed in **Erreur! Source du renvoi introuvable.** following the nomenclature exposed in Figure 3.

Table 2 – Formulas for water volume variation estimation between two states

Power law	$\Delta V = c(H_2^d - H_1^d)$
Heron's formula	$\Delta V = \frac{1}{3}\left(A_1 + A_2 + \sqrt{A_1 * A_2}\right) * \Delta H$
Mean area	$\Delta V = \frac{1}{2}(A_1 + A_2) * \Delta H$
Basic volume (for unvarying lake areas)	$\Delta V = A * \Delta H$ where *A* corresponds to the unvarying surface extent of a lake
Integration	$\Delta V = \int_{H_1}^{H_2} f(H)\, dH \quad or \quad \int_{A_1}^{A_2} f(A)\, dA$

⇨ These five approaches will be tested during the planned benchmarking exercise for established hypsometric curves. The main criterion for evaluation during the planned exercise will be the precision of the volume variation estimation depending on the approach chosen for water volume variation estimation between two states. The establishment of the required hypsometric curve is described in section 2.2.

2.2 Hypsometric curve estimation

2.2.1 Hypsometry from geomorphic processes

Hypsometry (from Greek ὕψος, hupsos, "height" and μέτρον, metron, "measure") is the measurement of land elevation and depth of features of the Earth's surface relative to mean sea level). In the original paper on this topic in 1952, Arthur Strahler proposed a curve containing three parameters to fit different hypsometric relations:

$$y = \left[\frac{d-x}{x} \cdot \frac{a}{d-a}\right]^z$$

where *y* is the relative height, *x* the relative area, and *a*, *d* and *z* the fitting parameters.

Differences in hypsometric curves arise from geomorphic processes that shape the landscape (Strahler 1952; Ohmori 1993; Wilgoose & Hancock 1998; Harsha et al., 2020; Zhang et al., 2020). The non-dimensional hypsometric curve provides a hydrologist or a geomorphologist with a way to assess the similarity of watersheds — and is one of several characteristics used for doing so. Applied to the lakes, the hypsometry curve may induce the estimation of lake geometry and potential classification (Håkanson 1977). The geomorphic processes occurring within basins and landforms are analyzed with the hypsometric curve of the basin which is the non-dimensional measure of the proportions of surface area of a catchment or watershed above a given elevation (Willgoose and Hancock 1998). Hypsometric curves assist in investigation of erosion stage of the basins and the lithology controlling the erosion in basin; and

provide valuable information about the basin slope and geomorphology of the basin, which finds applications in watershed treatment, basin planning and identification of rainwater harvesting structures (Sarp et al. 2011).

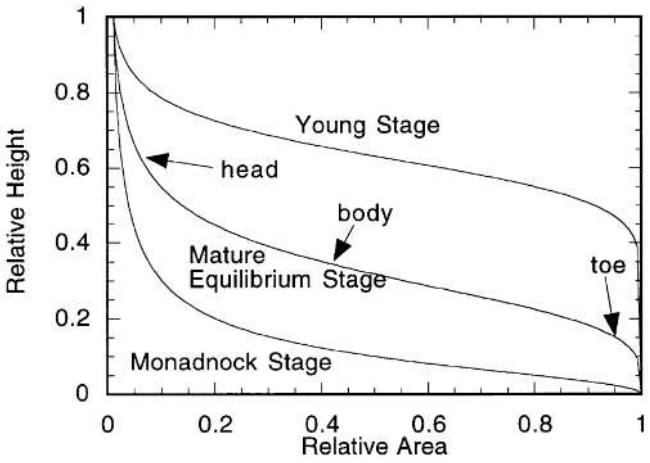

Figure 4 – Hypsometric curves classification (from Wilgoose & Hancock 1998)

2.2.2 Hypsometry from altimetry & surfaces

A hypsometric curve depicts the relationship between lake surface area and depth (or water level) and to calculate total lake volume (or lake storage change).

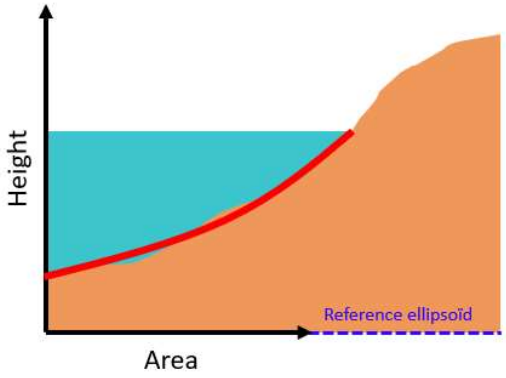

Figure 5 – Principle of hypsometric curve (estimated in red) for lake studies

Magome et al. (2004, 2006) explored the feasibility of determining water storage variation in lakes and reservoirs using 7 different methodologies. Using remote sensing data, from altimetry to DEM to imaging satellites, they managed to provide water storage variations in twelve lakes of Africa. They notably linked the area-height relation through a power law fitting. The volume variation from height and area estimations (from Topex/Poseidon and MODIS respectively) are then integrated from the H-A curve. This is, hidden but there, an approximation of the hypsometric curve linking height and area.

From various altimetry missions and LANDSAT images, estimation of the Nasser Lake volume variations has been made in Abileah et al. 2011. By setting the hypsometric curve by fitting the water height from altimetry and water surface extents from Landsat points over the lake, the derivation of water volume variation from the measured lowest water level has been made for the 1992-2011 period. Along with this volume estimation, the 10m-height variation observed between 1998 and 2004 led to an estimation of the bathymetry for the lake's borders.

Following the previous results on lake volume estimation exposed in Crétaux et al., 2011, and the survey of reservoirs and lakes from remote sensing for the Syrdaria basin (Crétaux et al., 2015) a study of the Tibetan Plateau (TP) lakes is done in Crétaux et al. (2016). They use a mix between water surface extents from optical data and water height from satellite altimetry. The purpose is to link the impact of climate change with the observed rise in water level (and hence volume) in the TP. They produced, for each lake, a 2nd-order polynomial linking lake surface extent to height (the hypsometric curve). They then derive the water volume variation using the Heron formula, and observe a rising trend in water volume estimation for the TP. The addition, compared to Duan & Bastiaanssen 2013, is that the lakes are smaller, and that the hypsometric equation can be extrapolated. The relation between surface extent and volume seems almost linear (slightly bent). The technique is applied and distributed online on the Hydroweb website (see section 4.1), which estimates volumes around 100 lakes worldwide. Yet no solution is proposed for smaller lakes located outside the altimetry track.

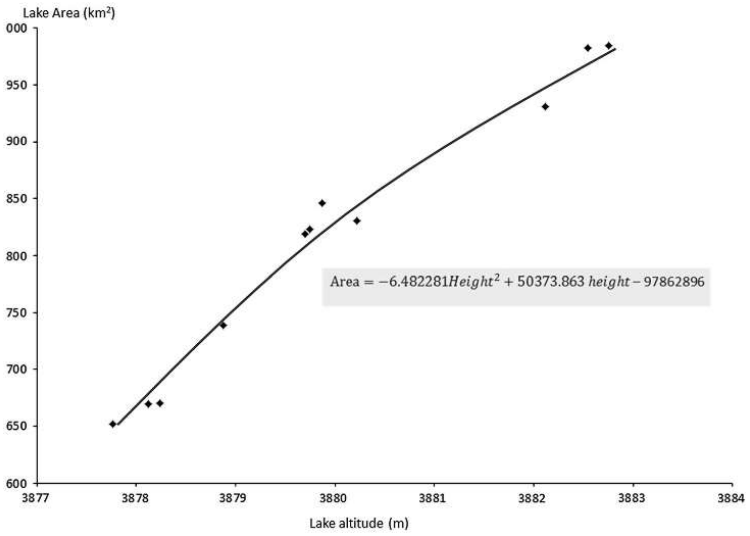

Figure 6 – Hypsometry polynomial of Lake Ayakkum (within the hypsometry equation, height is expressed in meters and area in km²) (from Crétaux et al., 2016)

In Busker et al. 2019, time series of variation in lake and reservoir volume between 1984 and 2015 were analyzed for 137 lakes over all continents by combining the monthly JRC Global Surface Water (GSW – Pekel et al. 2016) dataset from 1984 to 2015 and the satellite altimetry database DAHITI. Lake areas and water levels were combined in a regression to derive the hypsometry relationship (dh/dA) for all lakes. Nearly all lakes showed a linear regression, and 42 % of the lakes showed a strong linear relationship with a $R^2 > 0.8$, an average R^2 of 0.91 and a standard deviation of 0.05. A similar methodology is proposed in Schwatke et al. 2020, with an estimation of the hypsometric curve derived from Strahler 1952 (see previous section 2.2.1) for the water surface extent/height point from altimetry and optical imagery with the DAHITI database. They indeed propose to use a mmodified Strahler approach to estimate the hypsometric curves for lakes and reservoirs as follows:

$$y = \left[\frac{(x_{min} - x)}{(x_{min} - x_{ip})} . \frac{(x_{max} - x_{ip})}{(x_{max} - x)}\right]^z . y_{scale} + y_{min}$$

This derived Strahler equation relies on the lake depth assumption from Cael et al. 2017. This means that they used the area-depth relationship from this study (derived from the Hurst coefficient) to define rough limits for the minimum water level y_{min}. This methodology might introduce errors as the estimation of the maximum depth remains tricky, leading to biases in the LSC estimations. This should be explored though.

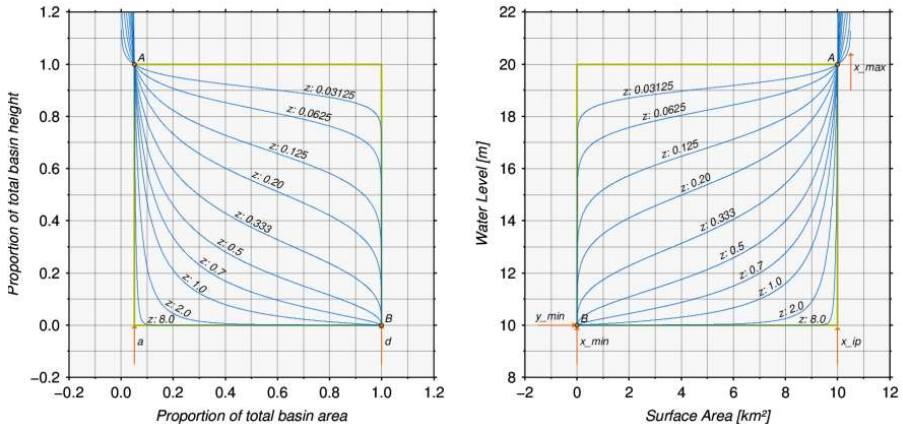

Figure 7 – Original Strahler approach (left) and modified Strahler approach based on water levels and surface areas (right). (from Schwatke et al. 2020).

Either surface area can be expressed as a function of height, or reversely. In the case of hypsometric curve estimation, the surface areas as well as the heights correspond to independent observations with biases and/or errors. Heights and surface extents might thus be considered as data pairs and must be estimated at the same time for the estimation of the hypsometric curve to represent precisely one lake state (i.e. coherent water height-area relationship). One solution could be a least squares approach with a Gauss-Helmert compensation and RANSAC algorithms.

In the Lakes_CCI project, Lake Water Extent (LWE) is derived from the Lake Water Level ECV product (LWL) with a hypsometric curve which is estimated by least square adjustment of LWE-LWL vectors, the coefficients representing the linear relationships through polynomia of the first to 3rd order. Please refer to the ATBD of LWE for more details in [R1].

⇨ When the area-height couples are established from water height and surface extent estimations, the hypsometric curve can be estimated from various approaches. In the planned benchmark exercise, polynomials of first, second and third order will be compared with modified Strahler approach for the observation area and height spans. The use of a Gauss-Helmert compensation and RANSAC algorithm might also be explored.

2.3 Water level estimation

2.3.1 Altimetry water height estimation

Spatial altimetry allows the measurement of water level in rivers, lakes and flood plains. Since the early 1990s, several altimetry satellites have been launched, as shown in Figure 8. Their main objective is to measure ocean height, but their altimetry measurements can also be used to measure continental water levels (inland seas, rivers, lakes, flooded areas, reservoirs). The products are an important complement or even an alternative to in situ measurements, especially in regions where ground-based networks are either non-existent or disappearing. Used in conjunction with other hydrological data and hydrological model outputs, these data make a valuable contribution to the study of the water cycle and the quantification of water resources. In this study, we will use all water level data available: HydroWEB including Lakes_cci LWL data, DAHITI and G-REALM.

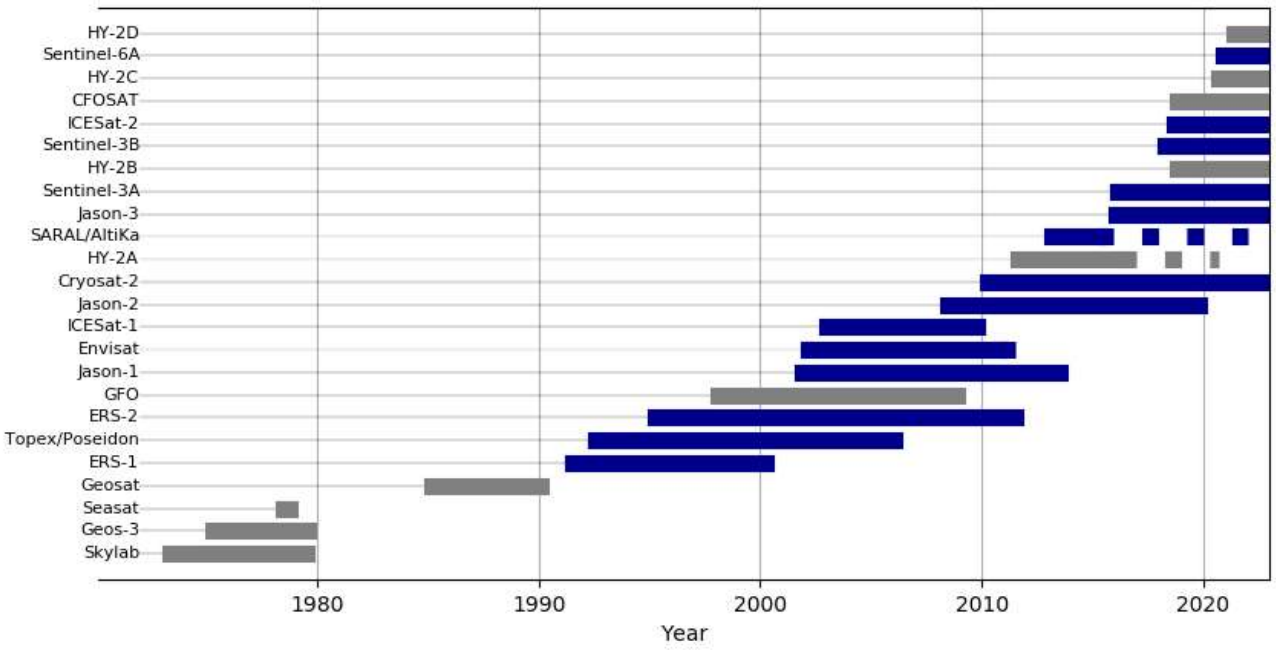

Figure 8 - Timeline for satellite altimeters. Dashed lines correspond to major orbit change. Blue lines correspond to altimeters used for continental hydrology purposes.

2.3.1.1 HydroWEB

With the HydroWEB service (http://hydroweb.theia-land.fr – Crétaux et al., 2011) hosted on the platform of the national French THEIA cluster and operated by CLS, LEGOS-CNES has been developing, since 2003, a database of water level variations on lakes and rivers around the world based on satellite altimetry. As of March 2023, 12,546 virtual stations are monitored on rivers and 442 on lakes, all available in HydroWEB, in operational mode (real-time update) or in delayed mode. In addition, changes in extent and volume are also measured for some of them. These observations allow the construction of long time series of water levels over continental surface waters.

This database includes the Lakes_CCI water level time series.

2.3.1.2 DAHITI

The Database for Hydrological Time Series of Inland Waters (DAHITI) was developed by the Deutsches Geodätisches Forschungsinstitut der Technischen Universität München (DGFI-TUM) in 2013 to provide water level time series of inland waters Schwatke et al. (2015). Today, DAHITI develops a variety of hydrological information on lakes, reservoirs, rivers, and wetlands derived from satellite data, i.e., from multi-mission satellite altimetry and optical remote sensing imagery. As for Hydroweb, all products are available free of charge for the user community after a short registration process.

As of March 2023, DAHITI currently provides 10 103 water level time series distributed over all continents, except Antarctica. In Africa (2082 time series), Asia (1737), Australia (46), Europe (680), North America (1395), and South America (4024) water level time series are available. 8,637 of these virtual stations follow rivers, 1,058 lakes and 387 reservoirs.

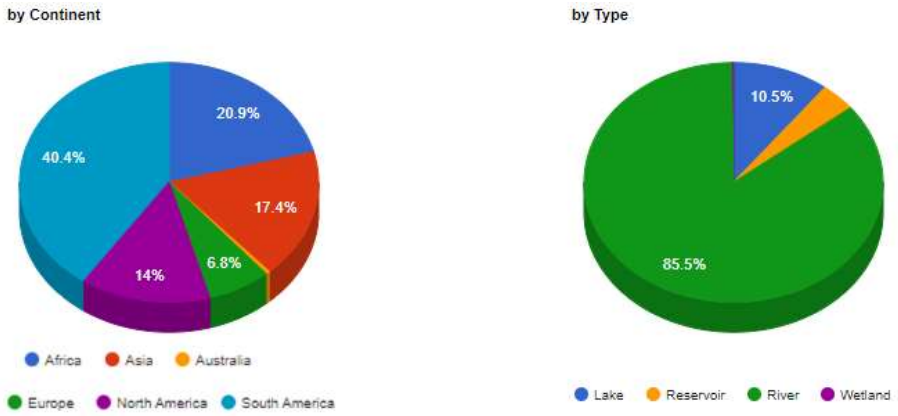

Figure 9 – Statistics on the DAHITI database of virtual stations, by continent and by types (as of March 2023)

2.3.1.3 G-REALM

The U.S. Department of Agriculture's Foreign Agricultural Service (USDA-FAS), in co-operation with the National Aeronautics and Space Administration, and the University of Maryland, are routinely monitoring lake and reservoir height variations for many large lakes around the world. This program is called Global Reservoir and Lake Monitoring (G-REALM) (Birkett & Beckley 2010). It utilizes NASA/CNES/ESA/ISRO radar altimeter data over inland water bodies in an operational manner. The surface elevation products are produced via a semi-automated process and placed on the G-REALM website for USDA and public viewing.

As of November 2022, 530 lakes are monitored, and their water height time series can be viewed and downloaded at *https://ipad.fas.usda.gov/cropexplorer/global_reservoir/*.

2.3.2 Water elevation from Digital Elevation Model

Two methodologies are explained here. The first uses Digital Elevation Model (DEM) produced with the lowest observed water level, representing the geomorphological topography of the watershed as much as is possible from observation data. The second supposes that the lake bathymetry can be inferred from its immediate surroundings. With those two ideas in mind, the use of DEM and their accuracy are key entries to estimate a lake LSC time series. We hereby present some studies using these approaches to determine watershed and lake volume from DEM.

In Amitrano et al., 2014, an innovative method is proposed to determine watershed volume estimation from SAR data in the Sahel area. They use COSMO-Skymed high-resolution data to first create a local DEM (using interferometry) when the water level is at its lowest (first methodology). Then, they detect the watershed surface using a De Gandi filter on multitemporal data, and then applying a threshold determined manually using the local histogram of the SAR data. To improve the water surface estimation, they apply a mode filter to the water body extracted made previously with the thresholding, followed by a morphological filtering (Ronse & Serra, 2013). The shoreline is estimated applying a Roberts operator (Shrivakshan and Chandrasekar, 2012). Once the shoreline is properly determined, the water volume contained into the basin can be computed considering each pixel of the water mask as a water column whose height h_{wc} is given by $h_{wc} = h_c - h$, where h_c is the elevation of the equipotential surface identified by the basin contour derived from the SAR intensity maps, and h is the DEM height corresponding to the considered pixel. Therefore, the water volume contained into the basin is given by the summation of all the elementary contributions brought by the water columns.

As the quality of the estimated volume depends highly on the DEM, the key element in this process is the quality of the DEM created or used to this purpose. This might be an issue in some cases, as many DEMs have not been produced at a low water level and are provided at low resolution. If the methodology developed in Amitrano et al. 2014 relies on SAR data, it can also be used for optical data for the s horeline height estimation, as done in Vanthof and Kelly 2019 using the NDWI.

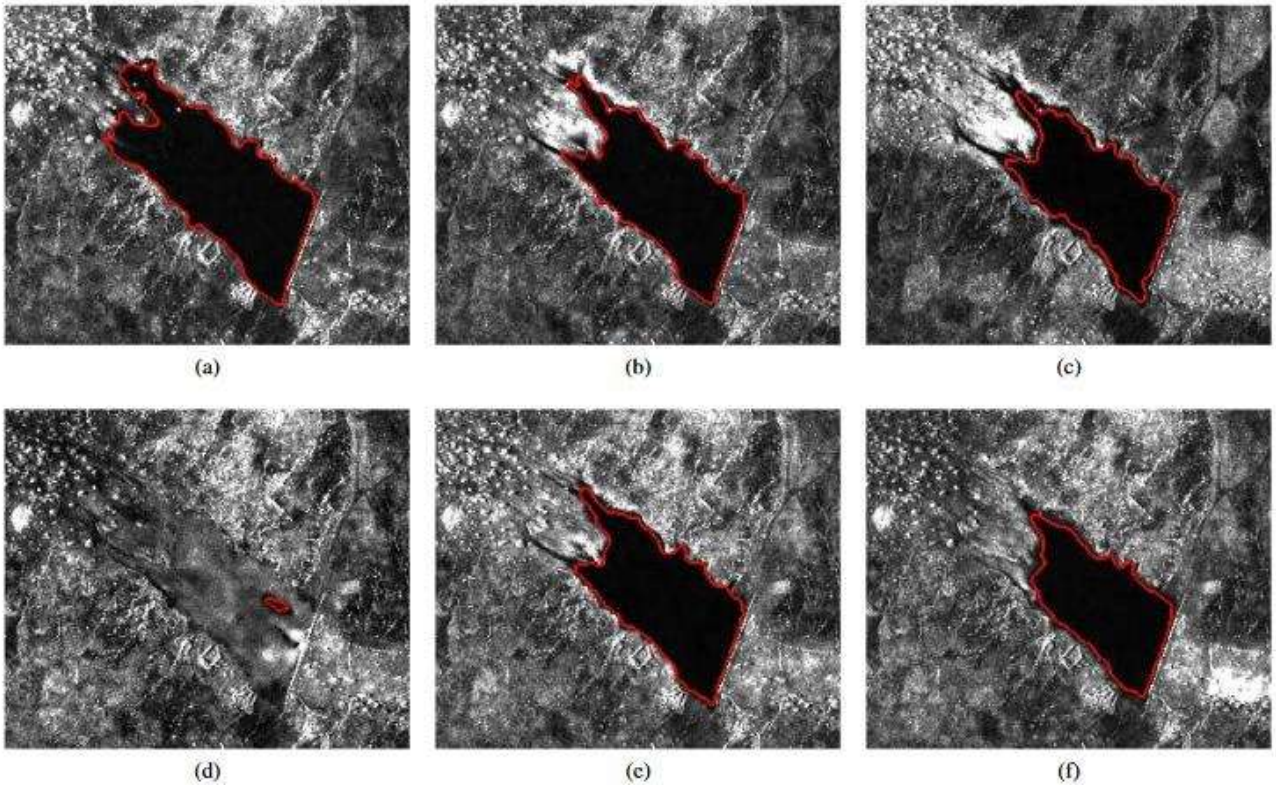

Figure 10 - Shoreline of the Laaba basin for six different dates (from Amitrano et al. 2014)

If the former study represents a typical pipeline for water volume estimation from either SAR or optical data, it needs an a priori knowledge of the waterless DEM (bathymetry). With freely accessible SAR SLC data, only Sentinel-1 would be a proper candidate. Nevertheless, the baseline between two acquisitions for similar orbits remains low for Sentinel-1, which helps monitor Earth's surface movements, but lead to poorly precise DEM estimation using interferometry. Such an approach cannot be easily proposed for all lakes at a global scale and specifically in the framework of this study. This is due to the use of high-resolution DEM (without water if possible) with private COSMO-Skymed data that are not in our possession or freely accessible. However, the approach for accessible DEM with lower resolution will be tested, as it is promising for ungauged lakes and reservoirs.

A global approach has already been exposed in section 2.1.2 with the work proposed in Messager et al. 2016 (hydrolakes database + derived databases and products like GLOBathy). In this work they related the surrounding topography of lakes and reservoirs to their estimated bathymetry. If the approach might be suitable for reservoirs with an acceptable error margin, natural lakes might present "surprising" results compared to their surroundings, with deep maximum depth in almost planar areas.

Using a multiple-year drought in NorthEastern Brazil, Zhang et al. 2021 produced a "dry" DEM using data from TanDEM-X acquired at this time. Mixing the bathymetry information produced this way with high resolution contours of the water bodies from RapidEye between 2009 and 2017, they managed to produce the A-V-E curves, and thus to follow the water variation at a regional scale on 2140 reservoirs.

⇨ All available water level from altimetry will be considered in the planned benchmark exercise. Concerning the use of DEM to map the water surface and retrieve water level, we will compare the "classic" approach with altimetry on lakes where we have access to high-resolution DEM and also explore the use of global and freely DEM (Copernicus, MERIT and Fabdem) on several lakes to analyse the feasibility and understand the current potential limitations for global studies (the Renaissance dam for instance).

2.4 Water surface extent estimation

Lake water surface extent estimations are used for 2 different purposes:

1 - To compute the hypsometric curve

2 - To estimate at a certain date the lake storage change from both its extent and an already established hypsometric curve.

For the first purpose, a monthly water bodies database could be sufficient, but specific processing is needed for the direct estimation of LSC from lake water extent if no pre-calculated dataset is used. In the planned benchmarking phase, we will explore the impact of different water surface extent datasets available on both the hypsometric curve estimation and its use for LSC estimation.

This question of water surface extent (WSE) is also considered in the baseline of the Lakes_cci project as it is a Lake ECV product. We won't use the LWE dataset of the Lakes_cci product as it is derived from Lake Water Level (LWL) data and a hypsometric curve (see [R1] for details). We will use the LWL-LWE vector data used to retrieve the hypsometric curve in the benchmark to assess the other methodologies.

In addition to these data from the baseline, the following sub-sections describe 2 types of data, dynamic data, and static data, that can be used for the benchmark and indicate also what should be considered in the benchmark.

2.4.1 Dynamic approaches

2.4.1.1 Optical indices

In remote sensing, indices are part of the processing methods called multispectral transformations. They consist in converting luminance measured at the satellite sensor into quantities that have a meaning in the environment. Based on the multispectral character of satellite data, they can describe the state of a phenomenon.

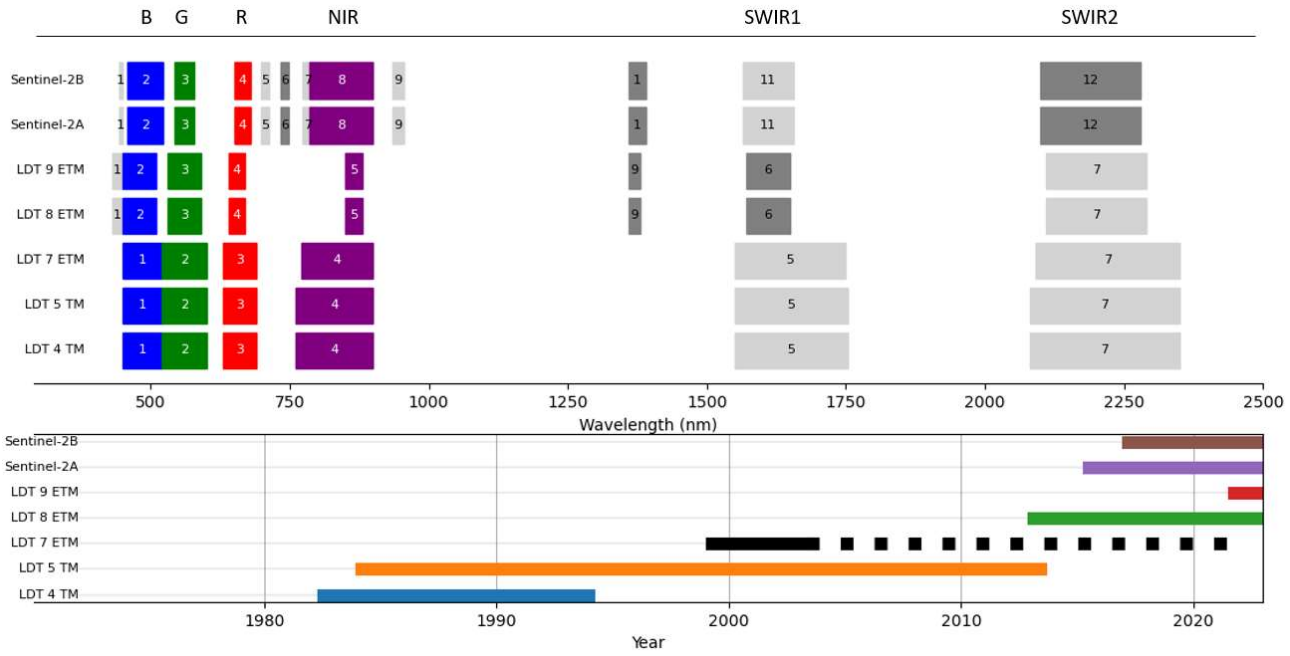

Figure 11 - Band availability and lifespan of the main optical satellites. Landsat 7 experienced from 2003 a sensor incident that deteriorated strongly the data acquisition (dashed line).

All indices, whether vegetation indices, soil indices, or water indices for our matter, are based on an empirical approach based on experimental data. Through the years and the improvement of remote sensing technologies, precision, and increasing number of available bands, many indices were proposed to estimate water surface areas. The main indices dedicated to water detection are listed in Table 3. Usually made to have values between -1 and 1, they lead to the production of rasters which highlight the presence of water. You can observe on **Erreur ! Source du renvoi introuvable.** such indices produced on the Bankim reservoir lake (Cameroon).

Table 3 - List of optical indices used for water detection.

Index	Expression	Reference paper
TCwet	$TC_{wet} = 0.1509 * B + 0.1973 * G + 0.3279 * R + 0.3406 * NIR - 0.7112 * SWIR1 - 0.4572 * SWIR2$	Crist 1985
NDWI - Normalized Difference Water Index	$NDWI = \frac{NIR - SWIR}{NIR + SWIR}$	McFeeters 1996
MNDWI - Modified Normalized DifferenceWater	$MNDWI = \frac{G - SWIR}{G + SWIR}$	Xu 2006
AWEI – Automated Water Extraction Index	$AWEI_{nsh} = 4 * (G - SWIR1) - (0.25 * NIR + 0.75 * SWIR2)$ $AWEI_{sh} = B + 2.5 * G - 1.5 * (NIR + SWIR1) - 0.25 * SWIR2$	Feyisa et al. 2014
NWI – New Water Index	$NWI = \frac{B - (NIR + SWIR1 + SWIR2)}{B + (NIR + SWIR1 + SWIR2)}$	Yang & Du 2017
MBWI	$MBWI = 3 * G - R - NIR - SWIR1 - SWIR2$	Wang et al. 2018

The use of indices derived from optical data do suffer from at least five different sources that do not lead to an automatic and reliable use for water surface extent estimation:

- Obviously the first source of error is the correct detection of clouds. If not properly detected, as they are made of water drops, they might be misclassified as water areas.
- Sometimes related to the previous source of error, the shadowed areas with low luminance can bring interpretation issues. From clouds or from mountains, shadows are particularly tricky to process, and might have the strongest impact at high latitudes.
- Vegetation is also a not negligible source of misclassification. Either floating on the water surface (macrophytes) or covering the shores from surrounding trees
- Other floating objects on water (boats, houses, fisheries mainly), as can be observed on Figure 12
- The confusion between water and snow cover may also induce over detections (Khalid et al. 2021)

A manual thresholding is often used to semi-automatically detect water surface. It can be supervised from Landsat data on derived indices, generally the NDWI (Annor et al. 2009; Peng et al. 2006; Vanthof & Kelly 2019), the MNDWI (Duan & Bastiaanssen 2013), or both (Crétaux et al. 2015).

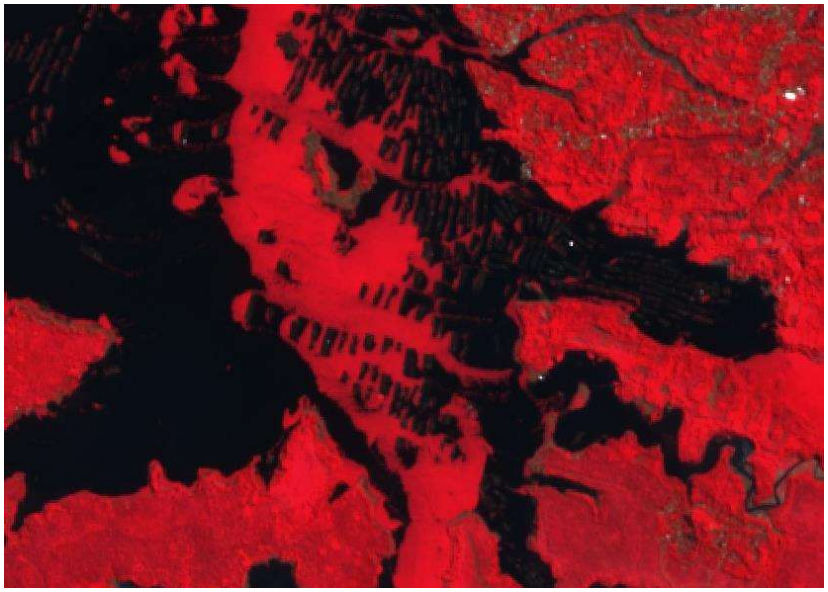

Figure 12 – Lake Waduk Cirata (Indonesia), here depicted in false colours from Sentinel-2 with red areas corresponding to vegetation. It presents floating vegetation, houses and fishery ponds on its surface, that make it difficult to precisely determine the lake water surface.

All these error sources lead to some issues in water surface delineation from water indices. The water areas are generally chosen for areas presenting values below or above a particular threshold, that may change from one date to another. This threshold is manually set or chosen through different approaches that are explored in the following sections.

⇨ Even if there are limitations on the use of these numerous indices approaches, the impact on LSC estimation has not been assessed and will be tested in the planned benchmark exercise. Moreover, it is not easy to get in situ data of water extent and testing several methodologies might improve the consistency of the work by giving the same trends.

2.4.1.2 Dynamic thresholding applied to optical indices

Donchyts et al. 2016 describes a dynamic thresholding method from several image processing methods: the Canny edge detection and the Otsu thresholding method applied to the MNDWI (see Figure 13**Erreur ! Source du renvoi introuvable.**). The spectral properties of water change with region, basin, and time. Often water is only a small part of the image, so thresholding to zero can introduce errors in area detection. The histogram-based Otsu thresholding method (Otsu, 1979) works very well on bimodal histograms; however, water sometimes represents only a small peak on the histogram. To circumvent this problem, a Canny edge detection filter is first used. Created in 1986 by Canny, (Canny, 1986), it is based on the following principle: the reduction of the image noise by Gaussian smoothing, an intensity gradient calculation, then the calculation of the orientation of the contours. The non-maxima values are then removed, and then the contours are thresholded by hysteresis. The contours are generally located where there is an abrupt change in value, which is generally the case around the basins on the hydrology indices. These contours are thickened by dilation and then the Otsu thresholding is applied on the index values corresponding to the created buffer. This time, the histogram shall present a bimodal histogram, which allows to recover a proper threshold valued. The Otsu method corresponds to a statistical method based on histograms: it searches between two classes for the k value of the histogram that best separates them according to the probabilities of belonging to these classes. The index is then thresholded with this k value to obtain the water mask. Thus, this method has the advantage of adapting itself according to the image, so we are free from the potential errors that could result from a thresholding to a fixed zero value. It allows to approach the automation of the surface detection algorithm.

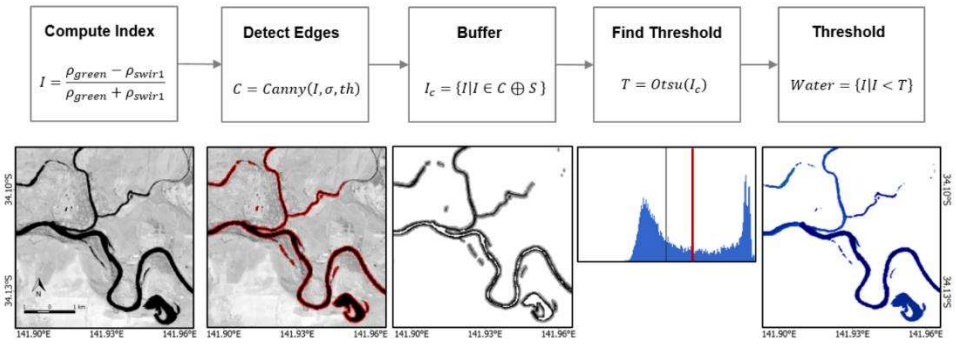

Figure 13 - Principle of Otsu Sequencing on contours (from Donchyts et al., 2016)

⇨ This methodology will be interesting to test. However, as the codes work on the Google Earth Engine with proprietary libraries, CLS has recoded and enhanced it to multiple indices.

2.4.1.3 Multi-index approaches

If former studies used manually supervised approaches using optical indices to determine water surfaces, an increasing number of approaches propose semi or totally automatic methodologies to estimate these surfaces.

Feng et al. 2016 developed an automated method for mapping inland surface water bodies by combining coarse-resolution, global estimates of water cover with high-resolution estimates of surface reflectance and topographic indices. The water detection methodology relies strongly on a decision tree using NDWI and MNDWI along with NDVI, with static thresholds. The method has been implemented with open-source libraries to facilitate processing large amounts of Landsat images on high-performance computing machines. With the support of the computing environment at the Global Land Cover Facility (GLCF), the method has been applied to the roughly 9,000 Landsat scenes of the GLS 2000 data

collection to produce a global, 30-m-resolution inland surface water body dataset (GIW) for circa-2000. Though the results provide a satisfactory water body dataset, it is a static one produced on one dataset, the GLS 2000 data collection (see Figure 14).

In Cordeiro et al. 2021, they propose an alternative detection method via unsupervised classification. For this they compute for a particular image the MBWI, on which they run a hierarchical clustering. Clusters are formed based on their Euclidean distance and linkage ("average linkage"). The ideal number of clusters is chosen according to the variance ratio criterion. Finally, the cluster corresponding to water is selected by identification with the highest MBWI value. This method is repeated several times to find the ideal number of groups. To reduce the processing time, a naive Bayes classifier is used to choose the best model from a few pixels of the image. This algorithm has been enhanced by CNES to become the SurfWater algorithm.

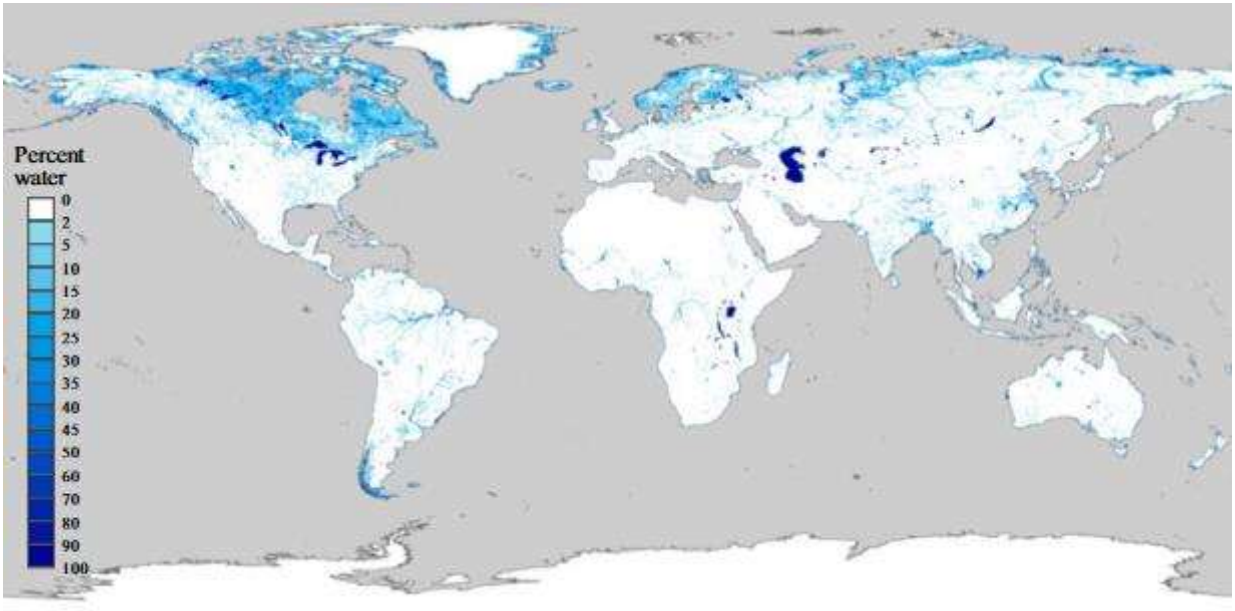

Figure 14 - Global water data derived from the 8,756 Landsat ETM+ images in the GLS2000 dataset (from Feng et al., 2016)

In Schwatke et al. 2019, they use Sentinel and Landsat data. The data are first pre-processed to create cloud-free level 3 images. The images are then merged band by band. Five indices are used: MNDWI, NWI, AWEInsh, AWEIsh and TCW. The histograms (cumulative and non-cumulative) are computed to perform a thresholding. A first threshold at 0 on the MNDWI is arbitrarily fixed, we search via the histograms of the other indices the associated pixel and value. This search is done in a window of data defined by an interval, which allows to get rid of the noise of the histogram. Finally, the defined thresholds are averaged and the images thresholded according to this value. The main advantage of this methodology is the robustness through the multiplicity of indices, as well as the adaptation of this threshold value. The MNDWI thresholded at a value of zero is only used for basic thresholding for the other indices. Nevertheless, the pre-processing of the input data is consequent, and the histogram processing is computationally time consuming. Furthermore, some parameters are not known, and some processing steps are calculated on Google Earth Engine. These points prevent a proper evaluation of the algorithm itself, but the time series produced on the test lakes will be explored.

⇨ For the benchmark phase, the time series of lake's surfaces following the approach of Schwatke et al. (2019), Surfwater will be assessed, when available, with the other surface areas products for the estimation of the hypsometric curve and its impact on Lake Storage Change estimation.

2.4.2 Static data: the Global Surface Water dataset

2.4.2.1 GSW methodology to retrieve water extent

Using more than 30 years of 30m Landsat data, the JRC proposes the Global Surface Water (GSW) dataset (Pekel et al. 2016). The entire archive of the Landsat 5 Thematic Mapper (TM), the Landsat 7 Enhanced Thematic Mapper-plus (ETM+) and the Landsat 8 Operational Land Imager (OLI) orthorectified, top-of-atmosphere reflectance and brightness temperature images (L1T) acquired between 16 March 1984 and 10 October 2015 was used. Since 2016, they regularly produce monthly dataset from 1984 until now. GSW changed everything as a static dataset and is an absolute reference in terms of water surface studies. For more details about the methodology to produce this dataset, please refer to Pekel et al. 2016 or the explanation put in Appendix B -.

2.4.2.2 GSW dataset use for LSC estimation

Following the work initiated in Pekel et al. 2016 with the GSW dataset, Khandelwal et al 2022 created the ReaLSat database of reservoir and lake surface area variations. This new global dataset contains the location and surface area variations of 681,137 lakes and reservoirs larger than 0.1 square kilometres (and south of 50-degree N) from 1984 to 2015, to enable the study of the impact of human actions and climate change on freshwater availability. They produced time series of surface area and a shapefile containing monthly shapes for each lake. If the monthly scale pixel maps from the GSW dataset were accurate and complete, it would be straightforward to produce surface extent shapes at each timestep for individual lakes from these maps. However, these maps tend to suffer from large amounts of missing data and labelling errors. To address this, they used the ORBIT approach to correct GSW labels and impute missing labels using physics-based bathymetry constraints.

They extracted pixel-based water extent maps for each lake in the static lake polygon database at a monthly scale from GSW. Specifically, for a given lake, they created a bounding box around its static shape and extracted the monthly water extent maps. To avoid including other nearby lakes in the water extent maps, they only consider the water pixels connected to the target lake at least five times in the total time duration of 32 years. This step masks out pixels that may incorrectly connect the target lake with other nearby lakes. Each pixel in these water extent maps is labelled as either land, water, or missing. As mentioned earlier, these maps contain large amounts of missing labels and erroneous labels and thus require further processing to improve their quality.

⇨ In the benchmark phase, we will test the impact of the use of static data to generate the hypsometric curve and to the LSC estimation.

2.5 Perspectives on Bathymetry estimation for lake volume estimation

Access to the lake volume estimation and not only its variation needs to have an idea of the bathymetry. However, it is rarely available. The references hereafter summarise the different possibilities. Depending on the time available for this option, we could consider testing some approaches, especially with ICESAT.

A line of research since the 1990s is the estimation of lake and costal bathymetry using satellite optical data and/or altimetry. The huge advantage of getting precise bathymetry is that it directly leads to A-H-V curves or estimates (as in Khazaei et al. 2022 or Zhang et al. 2021). Practically, bathymetry

products are very scarce and expensive to produce, and thus their utilization is not generalized. Knowing that, some studies try to derive the bathymetry information from remote sensing data.

Sandidge & Holyer 1998 use data from the Airborne Visible/Infrared Imaging Spectrometer (AVIRIS) in a neural network system to establish quantitative, empirical relationships between one of these parameters, depth, and remotely sensed spectral radiance. They show that the ability of the neural network to generalize, producing algorithms with some degree of universality among diverse coastal environments is demonstrated. The result of the generalization analysis is of practical importance because it indicates that the neural network may not require an extensive training set of water depth data to be "tuned" for each location where depth retrievals are desired. However, the AVIRIS data are scarce and not publicly shared in general.

In Mohamed & Nadaoka 2017, they compare in-situ bathymetry datasets with estimations from two empirical approaches: Random Forest (RF) and Multi-Adaptive Regression Spline (MARS) in three different areas with different turbidities. It appeared that these two methods (RF and MARS) outperform the Lyzenga Generalyzed Linear model (GLM) and Neural Network model. The RF algorithm produces the most accurate results and proved to be a preferable algorithm for bathymetry mapping in the shallow water context. In Mohamed et al. 2017, they further the investigation by comparing the tree-fitting algorithm using bagging (BAG), the ensemble regression tree-fitting algorithm of least squares boosting (LSB) and support vector regression algorithm (SVR) with the NN and GLM models over the same three sites. Compared with the echosounder data, BAG, LSB, and SVR results demonstrate higher accuracy ranges from 0.04 to 0.35 m more than Lyzenga GLM. The BAG algorithm, producing the most accurate results, proved to be the preferable algorithm for bathymetry calculation.

In Arsen et al. 2013, they use the laser ranging altimeter ICESat (Ice, Cloud, and land Elevation Satellite) during lake Poopó (Bolivia) lowest stages to measure vertical heights with high precision over dry land. These heights are used to estimate elevations of water contours obtained with Landsat imagery. Contour points with assigned elevation are filtered and grouped in a points cloud. Mesh gridding and interpolation function are then applied to construct 3D bathymetry. Complementary analysis of Moderate Resolution Imaging Spectroradiometer (MODIS) surfaces from 2000 to 2012 combined with bathymetry gives water levels and storage evolution every 8 days. With the ICESat-2 satellite (since 2018) which has lowered its footprint diameter to 13m and Sentinel 1 and 2 data, there are good perspectives to apply this method for large and smaller lakes. A similar approach on the Sobradino reservoir combining Landsat imagery with water height information derived from IceSAT-2 to estimate the "observed" bathymetry and derive LSC estimation is proposed in Bacalhau et al., 2022.

Preparing the launch of the ICESat-2 mission, Li et al 2019 studied the use of an ICESat-2 airborne prototype called MABEL (Multiple Altimeter Beam Experimental Lidar) and Landsat historical data to produce bathymetry information on lake Mead. This preliminary work was followed by the work exposed in Li et al 2020, where they used both altimetry data (ICESat, G-REALM, Hydroweb) with water surfaces from the GSW and GRSAD datasets. They then produced bathymetry over 347 reservoirs worldwide. For unobserved area, they projected the bathymetry with relatively large uncertainties and errors. Once again working on lake Mead, Li et al. 2021 determine A-V-E curve using information from both GSW and TanDEM-X to obtain the visible bathymetry. They managed to add 3m of bathymetry depth using information on transitional water extracted from TanDEM-X data.

A similar approach proposed by Armon et al. 2020 enhanced these results over shallow lakes Eyre (Australia), El-Mellah (Algeria) and Coipasa (Bolivia), using ICESat-2 and the water occurrence from the GSW dataset. The methodology can be applied to a large portion of the shallow lakes around the world, enabling the mapping of inundated lakes, small lakes, and large and complex lake systems.

Finally, CLS and CNES are developing a deep learning approach to retrieve unknown bathymetry from already existing DEM. It relies on a virtual lake database. This database is formed from existing DEM (MERIT, CopernicusDEM) following the Hydrobasin delineations. After training the algorithm, from a lake-

filled" DEM the algorithm estimates a lake-"empty" bathymetry. It is currently at a R&D stage, but first results are promising, and the algorithm could be tested on some lakes/reservoirs with known bathymetry.

3 User requirements

The majority of Earth's accessible fresh surface water is stored in more than 100 million lakes and reservoirs, which serve as vital resources for an exhaustive list of critical ecosystem functions and human and animal habitats. Only 0.4% of all the freshwater available on Earth is at the surface level (Meybeck et al., 1995), which makes it a scarce resource essential to life, under a strong human-induced stress.

Beyond their coupled effects on weather and climate, the role of lakes in global hydrological and biogeochemical cycles is closely linked to their geometric characteristics of surface area, depth, volume of stored water and shoreline length (Winslow et al., 2014). Spatially explicit knowledge of all these characteristics is crucial for understanding and modelling a wide variety of Earth system processes and their interactions with the environment (water budgets, carbon or methane exchange rates, sediment trapping, heat fluxes, the cycle of pollutants and nutrients, as well as associated ecological processes such as lake productivity or food chain dynamics).

The annex to GCOS-200 (as expressed in ESA document ESA-EOP-SC-AMT-2021-26) defines lake storage change and its fluctuations as a key issue: "The volume of the lake water body is an integrator variable reflecting both atmospheric (precipitation, evaporation-energy) and hydrological (surface-water recharge, discharge and groundwater) conditions." The GCOS-240 status report indicates also "Water level, water extent and storage changes, surface water temperature (LSWT), ice phenology (ice-on/ice-off dates and ice duration) and water reflectance (water colour) are measured as part of an ESA Climate Change Initiative (CCI) project, Copernicus and NOAA.. They do mention for instance that information on changes in lake level and area is required on a monthly basis for climate assessment purposes. They also remind that approximately 95% of the volume of water held globally in approximately 4 000 000 lakes is contained in the 80 largest lakes. The dimensions in terms of frequency, resolution and required uncertainty and stability are not yet given for LSC.

The requirements for ECV datasets are expressed in terms of five criteria:

i) spatial resolution - horizontal and vertical (if needed).
ii) temporal resolution (or frequency) – the frequency of observations e.g., hourly, daily or annual.
iii) measurement uncertainty – the parameter, associated with the result of a measurement, that characterizes the dispersion of the values that could reasonably be attributed to the measurand.
iv) stability – the change in bias over time and quoted per decade.
v) timeliness - the time expectation for accessibility and availability of data.

In the latest Lakes_cci User Requirement Document (URD) [R2], a third user survey is presented. This addressed climate scientists, lake scientists and the wider scientific and expert user community interested in observing lakes. This survey collected feedback and requirements to align the project with user needs in Phase 2 of the project. It focused on the use of the dataset produced in Phase I. One question was "Do you need other thematic variables to be developed? (e.g., coefficient of extinction [Kd], Coloured Dissolved Organic Matter [CDOM], Forel-Ule colour index, Ice thickness, **Lake volume change**?)"

The 13 responses are reported in the following:

- Kd or Secchi depth maps would be very useful, as well as **Lake volume change**.
- Ice thickness, snow cover and Kd.
- Yes. CDOM would be very helpful.
- coefficient of extinction [Kd], ice thickness.
- All of the above.
- CDOM, Ice thickness, **Lake volume change**, possible other parameters on changes in lake morphology and biochemistry, e.g., ash and microplastics concentrations, greenhouse gases, especially methane.
- Information on water uses, withdrawals.
- Extinction coefficient and ice thickness (possibly snow thickness) would be very useful for modelling purposes. Then **lake volume change** is also of interest for hydrology and the water cycle.

- Kd.
- Yes, that would be very interesting, and it would probably enlarge the scope of use of the dataset.
- Dominant wavelength from chromaticity.
- CDOM would be very useful for our purposes.
- Coefficient of extinction [Kd], Ice thickness.

This shows that lake volume change is of interest for climate related hydrology and water cycle studies. The Centre National de Recherches Météorologiques (CNRM) has also shown such interest. They have a module for estimating the variation of some lake's volume in the frame of global modelling (FLAKE). They mentioned the difficulty to estimate the uncertainties in such variation estimations, but also mentioned that the accuracy of the lake's water volume was more important than the temporal cover in terms of modelling accuracy. This point was also shared with the JRC needs in terms of lake's volume variation. Some researchers also mentioned that for regional studies, data on as much lakes as possible is needed for an integrated approach, one lake alone being sometimes not enough to observe the climate change impact over time. Others have shown interest in being able to monitor such volume variations in remote areas.

In the end, the objective we have for the LSC product are as follows:

Spatial resolution	As many CCI lakes as possible
Temporal resolution	At least once per month
Uncertainty	<10% of total volume

4 Benchmark activities

The state of the art presented in this document showed many different methodologies to reach the purpose of estimating lake water content or variation. Among all the methodologies exposed, some will be tested in separate benchmarks to evaluate and choose the best techniques to be used for LSC estimation, both in terms of precision and efficiency. The benchmarks will focus on three main topics:

- Water height estimation from altimetry and from water surface area contours on DEM.
- Impact of water surface area estimation on hypsometric curve generation.
- Hypsometric curve estimation.
- Estimation of water volume variation from hypsometric curves.

Water height:

All available water level from altimetry will be considered in the benchmark. Concerning the use of DEM to map the water surface and retrieve water level, we will compare the classic approach with altimetry on lakes where we have access to the high-resolution DEM and explore the use of global and freely DEM (Copernicus, MERIT and Fabdem) on several lakes to analyse the feasibility and understand the current potential limitations for global studies (the Renaissance dam for instance).

Water surface areas impact on hypsometric curve:

It has been shown that the lake/reservoir surface is an unavoidable parameter when it comes to estimating the LSC between two dates. That is why different approaches will be explored, with a focus on their impact on the hypsometry curve and the derived LSC estimation. They will be tested on corresponding test lakes with as much validation data as possible. Global monthly static (GSW) and dynamic water surfaces (from the ESA CCI Phase 1&2 LWE, CNES's Surfwater algorithm, Donchyts-CLS adapted algorithm and lake surface's time series from DAHITI to enhance the consistency and confidence in the results) will be evaluated.

Hypsometry curve estimation:

When the area-height couples are established from water height and surface estimations, the hypsometric curve can be estimated from various approaches. In the benchmark, power laws, polynomials of first, second and third order will be compared for the observation area and height spans. The use of Gauss-Helmert and RANSAC algorithms will also be explored.

Volume variation estimation:

When the hypsometric curve is needed for the estimation of volume variations between two states, five different methodologies will be explored to evaluate the LSC variation. These are power laws, Heron's formula, the use of the mean area between the two states with the height difference, the basic volume variation (for non or low-varying surfaces), and finally the integration. We will also explore direct relationship of volume with surface and/or height and direct estimation of LSC.

5 Study sites

For test, validation and production purposes, a set of twenty lakes has been set up following various criteria. From the 63 candidates, 20 study lakes were selected around the world as can be observed on Figure 15. The selection criteria are as follows:

- All considered lakes had to be covered by altimetry measurements.
- All pedo-climatic areas had to be covered (i.e tropical, dry, temperate, continental, and polar).
- They had to show very low to very large area variations in time.
- Their maximum size had to show the largest panel possible.
- In-situ data had to exist to validate the LSC product; either area-height or volume-height relationships, bathymetry data (or empty DEM), height or surface or volume time series, or they had to be periodically empty.

Either published in scientific journals, shared publicly or privately, the validation datasets found on the final study lakes will help deeply in the pipeline setting, validation, and of course for the analysis of the LSC time series consistency (see Figure 16).

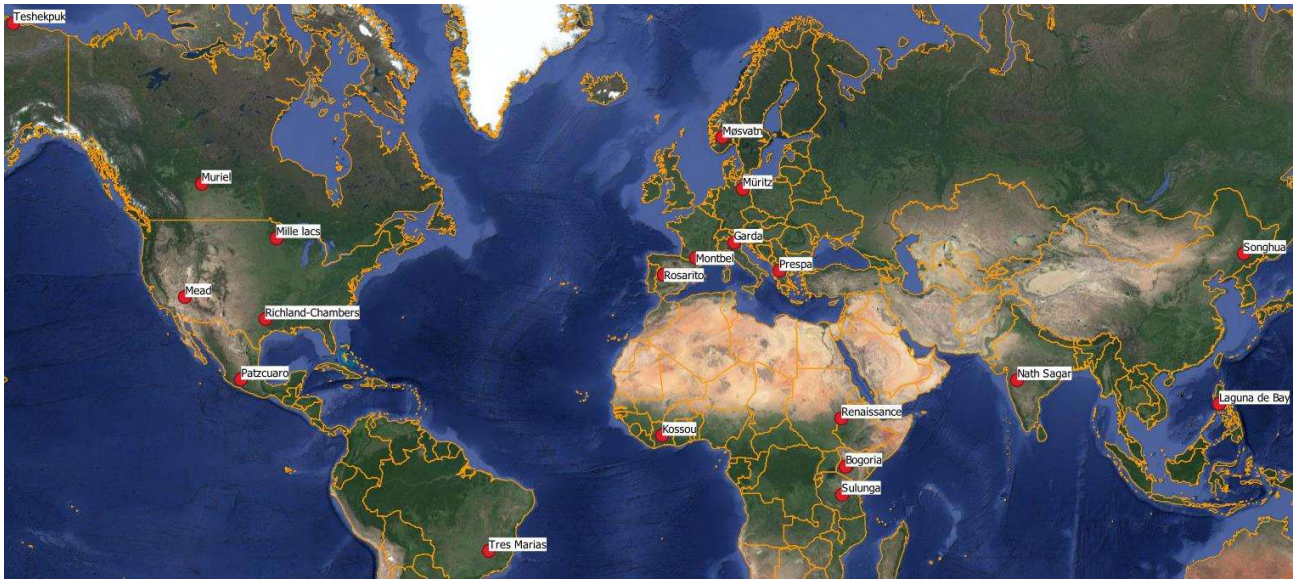

Figure 15 - Location of the twenty study lakes around the world

TEST LAKES

Country	Name	L or R?	Year built	Altimetry	Elevation (m)	Max size (km²)	Pedo-climatic areas (Köppen)					Surface variation variability	CCI?	Height and volume availability							Validation						Empty
														CCI lake		Hydroweb		Dahiti		GREALM	A-H	V-H	Bat.	TS			
							(A)	(B)	(C)	(D)	(E)			LWL	LWE	H	V	H	V	H				H	A	V	
Brazil	Tres Marias	R	1962	S3B	566	1040	1					Medium	1	1	1	1	1	0	0	0	X	X					
Canada	Muriel	L	n/a	S3A	555	64,1				1		Very low	1	0	0	0	0	1	0	0			X	X			
China	Songhua	R	1937	JA/S3A	243	550				1		Medium	1	1	0	1	0	1	0	1	X	X					
Ethiopia	Renaissance	R	2020	JA	450	1874	1					Very high	0	0	0	0	0	0	0	1			X				X
France	Montbel	R	1985	S3B	400	5,5			1			Very high	0	0	0	0	0	0	0	0			X	?	?	?	
Germany	Müritz	L	n/a	JA/S3B	59	117				1		Very low	1	0	0	0	0	0	0	0			X				
Greece Macedonia Albania	Prespa	L	s	S3A	841	259			1			Low	1	1	0	1	0	1	0	0					X	X	
India	Nath Sagar Jalashay	R	1976	S3A/S3B	460	350		1				High	1	1	1	1	1	1	0	0	X	X					
Italy	Garda	L	n/a	ENV/JA/S3B	62	370			1			Very low	1	1	0	1	0	1	0	0			X				
Ivory coast	Kossou	R	1972	S3A/S3B	185	1700	1					Medium	1	1	0	1	0	1	0	1				X			
Kenya	Bogoria	L	n/a	S3A	990	34	1					High	1	1	1	1	1	1	1	1			X				
Mexico	Patzcuaro	L	n/a	JA/S3B	2037	260			1			Low	1	0	0	0	0	0	0	1			X				
Norway	Møsvatn	R	1906	JA/S3B	919	79,1					1		1	0	0	0	0	1	0	0							
Philippines	Laguna de bay	L	n/a	S3B	2	911	1					Medium	1	0	0	1	0	0	0	0	X	X	X				
Spain	Rosarito	R	1958	S3B	306	15			1			High	1	0	0	0	0	0	0	0						X	
Tanzania	Sulunga	L	n/a	ENV/S3B	823	974		1				Very high	1	0	0	0	0	1	0	0							X
USA	Teshekpuk	L	n/a	S3A/S3B	9	830					1	Very low	1	0	0	0	0	1	0	0			X				
USA	Mead	R	1936	JA/S3A/S3B	372	640		1				High	1	1	0	1	1	1	1	1				X	X	X	
USA	Mille lacs	L	n/a	S3A/S3B	377	536				1		Very low	1	1	0	1	0	1	0	0			X				
USA	Richland-Chambers	R	1988	JA/S3B	97	168			1			Medium	1	0	0	0	0	1	1	0	X	X		X	X	X	

L: lake
R: reservoir
CCI? : present among the CCI-lake phase 2 2024 lakes
LWL: Lake Water level
LWE: Lake Water Extent
H: water height
A: water area
V: water volume estimation

Pedo-climatic areas (Köppen classification):
(A) Tropical
(B) Dry
(C) Temperate
(D) Continental
(E) Polar

A-H: Water Area-Height curve
V-H: Water Volume-Height curve
Bat.: Available bathymetry
TS: Time Series
Empty: lake periodically empty

Figure 16 - Test lakes and their description following the selection criteria

Appendix A - Bibliography

Abileah, R., Vignudelli, S., & Scozzari, A. (2011). *A Completely Remote Sensing Approach To Monitoring Reservoirs Water Volume*. 17.

Amitrano, D., Ciervo, F., Di Martino, G., Papa, M. N., Iodice, A., Koussoube, Y., Mitidieri, F., Riccio, D., & Ruello, G. (2014). Modeling Watershed Response in Semiarid Regions With High-Resolution Synthetic Aperture Radars. *IEEE Journal of Selected Topics in Applied Earth Observations and Remote Sensing*, *7*(7), 2732-2745. https://doi.org/10.1109/JSTARS.2014.2313230

Annor, F. O., van de Giesen, N., Liebe, J., van de Zaag, P., Tilmant, A., & Odai, S. N. (2009). Delineation of small reservoirs using radar imagery in a semi-arid environment : A case study in the upper east region of Ghana. *Physics and Chemistry of the Earth, Parts A/B/C*, *34*(4-5), 309-315. https://doi.org/10.1016/j.pce.2008.08.005

Armon, M., Dente, E., Shmilovitz, Y., Mushkin, A., Cohen, T. J., Morin, E., & Enzel, Y. (2020). Determining Bathymetry of Shallow and Ephemeral Desert Lakes Using Satellite Imagery and Altimetry. *Geophysical Research Letters*, *47*(7). https://doi.org/10.1029/2020GL087367

Arsen, A., Crétaux, J.-F., Berge-Nguyen, M., & del Rio, R. (2013). Remote Sensing-Derived Bathymetry of Lake Poopó. *Remote Sensing*, *6*(1), 407-420. https://doi.org/10.3390/rs6010407

Birkett, C. M., & Beckley, B. (2010). Investigating the Performance of the Jason-2/OSTM Radar Altimeter over Lakes and Reservoirs. *Marine Geodesy*, *33*(sup1), 204-238. https://doi.org/10.1080/01490419.2010.488983

Busker, T., de Roo, A., Gelati, E., Schwatke, C., Adamovic, M., Bisselink, B., Pekel, J.-F., & Cottam, A. (2019). A global lake and reservoir volume analysis using a surface water dataset and satellite altimetry. *Hydrology and Earth System Sciences*, *23*(2), 669-690. https://doi.org/10.5194/hess-23-669-2019

Cael, B. B., Heathcote, A. J., & Seekell, D. A. (2017). The volume and mean depth of Earth's lakes. *Geophysical Research Letters*, *44*(1), 209-218. https://doi.org/10.1002/2016GL071378

Canny, J. (1986). A Computational Approach to Edge Detection. *IEEE Transactions on Pattern Analysis and Machine Intelligence*, *PAMI-8*(6), 679-698. https://doi.org/10.1109/TPAMI.1986.4767851

Cooley, S. W., Ryan, J. C., & Smith, L. C. (2021). Human alteration of global surface water storage variability. *Nature*, *591*(7848), 78-81. https://doi.org/10.1038/s41586-021-03262-3

Cordeiro, M. C. R., Martinez, J.-M., & Peña-Luque, S. (2021). Automatic water detection from multidimensional hierarchical clustering for Sentinel-2 images and a comparison with Level 2A processors. *Remote Sensing of Environment*, *253*, 112209. https://doi.org/10.1016/j.rse.2020.112209

Crétaux, J.-F., Arsen, A., Calmant, S., Kouraev, A., Vuglinski, V., Bergé-Nguyen, M., Gennero, M.-C., Nino, F., Abarca Del Rio, R., Cazenave, A., & Maisongrande, P. (2011). SOLS : A lake database to monitor in the Near Real Time water level and storage variations from remote sensing data. *Advances in Space Research*, *47*(9), 1497-1507. https://doi.org/10.1016/j.asr.2011.01.004

Crétaux, J.-F., Biancamaria, S., Arsen, A., Bergé-Nguyen, M., & Becker, M. (2015). Global surveys of reservoirs and lakes from satellites and regional application to the Syrdarya river basin. *Environmental Research Letters*, *10*(1), 015002. https://doi.org/10.1088/1748-9326/10/1/015002

Crétaux, J.-F., Abarca-del-Río, R., Bergé-Nguyen, M., Arsen, A., Drolon, V., Clos, G., & Maisongrande, P. (2016). Lake Volume Monitoring from Space. *Surveys in Geophysics*, *37*(2), 269-305. https://doi.org/10.1007/s10712-016-9362-6

Crist, E. P. (1985). A TM Tasseled Cap equivalent transformation for reflectance factor data. *Remote Sensing of Environment*, *17*(3), 301-306. https://doi.org/10.1016/0034-4257(85)90102-6

Donchyts, G., Schellekens, J., Winsemius, H., Eisemann, E., & van de Giesen, N. (2016). A 30 m Resolution Surface Water Mask Including Estimation of Positional and Thematic Differences Using Landsat 8, SRTM and OpenStreetMap : A Case Study in the Murray-Darling Basin, Australia. *Remote Sensing*,

8(5), 386. https://doi.org/10.3390/rs8050386

Duan, Z., & Bastiaanssen, W. G. M. (2013). Estimating water volume variations in lakes and reservoirs from four operational satellite altimetry databases and satellite imagery data. *Remote Sensing of Environment*, *134*, 403-416. https://doi.org/10.1016/j.rse.2013.03.010

Feng, M., Sexton, J. O., Channan, S., & Townshend, J. R. (2016). A global, high-resolution (30-m) inland water body dataset for 2000 : First results of a topographic–spectral classification algorithm. *International Journal of Digital Earth*, *9*(2), 113-133. https://doi.org/10.1080/17538947.2015.1026420

Feyisa, G. L., Meilby, H., Fensholt, R., & Proud, S. R. (2014). Automated Water Extraction Index : A new technique for surface water mapping using Landsat imagery. *Remote Sensing of Environment*, *140*, 23-35. https://doi.org/10.1016/j.rse.2013.08.029

GCOS-200: The Global Observing System for Climate : Implementation Needs

Håkanson, L., & Hakanson, L. (1977). On Lake Form, Lake Volume and Lake Hypsographic Survey. *Geografiska Annaler. Series A, Physical Geography*, *59*(1/2), 1. https://doi.org/10.2307/520579

Harsha, J., Ravikumar, A. S., & Shivakumar, B. L. (2020). Evaluation of morphometric parameters and hypsometric curve of Arkavathy river basin using RS and GIS techniques. *Applied Water Science*, *10*(3), 86. https://doi.org/10.1007/s13201-020-1164-9

Hou, J., Van Dijk, A. I. J. M., Renzullo, L. J., & Larraondo, P. R. (2022). *GloLakes : A database of global lake water storage dynamics from 1984 to present derived using laser and radar altimetry and optical remote sensing* [Preprint]. ESSD – Land/Hydrology. https://doi.org/10.5194/essd-2022-266

Khalid, H. W., Khalil, R. M. Z., & Qureshi, M. A. (2021). Evaluating spectral indices for water bodies extraction in western Tibetan Plateau. *The Egyptian Journal of Remote Sensing and Space Science*, *24*(3, Part 2), 619-634. https://doi.org/10.1016/j.ejrs.2021.09.003

Khandelwal, A., Karpatne, A., Ravirathinam, P., Ghosh, R., Wei, Z., Dugan, H. A., Hanson, P. C., & Kumar, V. (2022). ReaLSAT, a global dataset of reservoir and lake surface area variations. *Scientific Data*, *9*(1), 356. https://doi.org/10.1038/s41597-022-01449-5

Khazaei, B., Read, L. K., Casali, M., Sampson, K. M., & Yates, D. N. (2022). GLOBathy, the global lakes bathymetry dataset. *Scientific Data*, *9*(1), 36. https://doi.org/10.1038/s41597-022-01132-9

Li, Y., Gao, H., Jasinski, M. F., Zhang, S., & Stoll, J. D. (2019). Deriving High-Resolution Reservoir Bathymetry From ICESat-2 Prototype Photon-Counting Lidar and Landsat Imagery. *IEEE Transactions on Geoscience and Remote Sensing*, *57*(10), 7883-7893. https://doi.org/10.1109/TGRS.2019.2917012

Li, Y., Gao, H., Zhao, G., & Tseng, K.-H. (2020). A high-resolution bathymetry dataset for global reservoirs using multi-source satellite imagery and altimetry. *Remote Sensing of Environment*, *244*, 111831. https://doi.org/10.1016/j.rse.2020.111831

Li, Y., Gao, H., Allen, G. H., & Zhang, Z. (2021). Constructing Reservoir Area–Volume–Elevation Curve from TanDEM-X DEM Data. *IEEE Journal of Selected Topics in Applied Earth Observations and Remote Sensing*, *14*, 2249-2257. https://doi.org/10.1109/JSTARS.2021.3051103

Liebe, J., (2002). Estimation of water storage capacity and evaporation losses of small reservoirs in the Upper East region of Ghana. Diploma thesis, Department of Geography, university of Bonn, Bonn.

Liebe, J., van de Giesen, N., & Andreini, M. (2005). Estimation of small reservoir storage capacities in a semi-arid environment. *Physics and Chemistry of the Earth, Parts A/B/C*, *30*(6-7), 448-454. https://doi.org/10.1016/j.pce.2005.06.011

Magome J., Hirano J., Takeuchi K., & Ishidaira H. (2006). GLOBAL MONITORING OF WATER STORAGE IN LAREGE LAKES AND RESERVOIRS BY SATELLITE OBSERVATIOS. *Proceedings of the Symposium on Global Environment*, *14*, 11-14. https://doi.org/10.2208/proge.14.11

Magome, J., Ishidara, H., & Takeuchi, K. (s. d.). *SATELLITE MONITORING OF WATER STORAGE VARIATION FOR WATER RESOURCES MANAGEMENT IN UNGAUGED BASINS*. 8.

McFEETERS, S. K. (1996). The use of the Normalized Difference Water Index (NDWI) in the delineation of open water features. *International Journal of Remote Sensing*, *17*(7), 1425-1432. https://doi.org/10.1080/01431169608948714

Meigh, J. (1995). The impact of small farm reservoirs on urban water supplies in Botswana. *Natural Resources Forum*, *19*(1), 71-83. https://doi.org/10.1111/j.1477-8947.1995.tb00594.x

Messager, M. L., Lehner, B., Grill, G., Nedeva, I., & Schmitt, O. (2016). Estimating the volume and age of water

stored in global lakes using a geo-statistical approach. *Nature Communications*, *7*(1), 13603. https://doi.org/10.1038/ncomms13603

Meybeck, M. (1995). *Global Distribution of Lakes. Physics and Chemistry of Lakes, 1–35.* doi:10.1007/978-3-642-85132-2_1

Mohamed, H., AbdelazimNegm, Salah, M., Nadaoka, K., & Zahran, M. (2017). Assessment of proposed approaches for bathymetry calculations using multispectral satellite images in shallow coastal/lake areas : A comparison of five models. *Arabian Journal of Geosciences*, *10*(2), 42. https://doi.org/10.1007/s12517-016-2803-1

Mohamed, H., Nadaoka. K. (2017). Assessment of Machine Learning approaches for bathymetry mapping in shallow water environments using multispectral satellite images. *International Journal of Geoinformatics* 13(2)

Ohmori, H. (1993). Changes in the hypsometric curve through mountain building resulting from concurrent tectonics and denudation. *Geomorphology*, *8*(4), 263-277. https://doi.org/10.1016/0169-555X(93)90023-U

Otsu, N. (1979). *A Threshold Selection Method from Gray-Level Histograms*.

Pekel, J.-F., Cottam, A., Gorelick, N., & Belward, A. S. (2016). High-resolution mapping of global surface water and its long-term changes. *Nature*, *540*(7633), 418-422. https://doi.org/10.1038/nature20584

Peng, D., Guo, S., Liu, P., & Liu, T. (2006). Reservoir Storage Curve Estimation Based on Remote Sensing Data. *Journal of Hydrologic Engineering*, *11*(2), 165-172. https://doi.org/10.1061/(ASCE)1084-0699(2006)11:2(165)

Ronse, C., & Serra, J. (2013). Algebraic Foundations of Morphology. In *Mathematical Morphology* (p. 35-80). John Wiley & Sons, Ltd. https://doi.org/10.1002/9781118600788.ch2

Sandidge, J. C., & Holyer, R. J. (1998). Coastal Bathymetry from Hyperspectral Observations of Water Radiance. *Remote Sensing of Environment*, *65*(3), 341-352. https://doi.org/10.1016/S0034-4257(98)00043-1

Sarp, G., Toprak, V., & Duzgun, S. (s. d.). *HYPSOMETRIC PROPERTIES OF THE HYDROLIC BASINS LOCATED ON WESTERN PART OF NAFZ*. 4.

Sawunyama, T., Senzanje, A., & Mhizha, A. (2006). Estimation of small reservoir storage capacities in Limpopo River Basin using geographical information systems (GIS) and remotely sensed surface areas : Case of Mzingwane catchment. *Physics and Chemistry of the Earth, Parts A/B/C*, *31*(15-16), 935-943. https://doi.org/10.1016/j.pce.2006.08.008

Schwatke, C., Dettmering, D., Bosch, W., & Seitz, F. (2015). DAHITI – an innovative approach for estimating water level time series over inland waters using multi-mission satellite altimetry. *Hydrology and Earth System Sciences*, *19*(10), 4345-4364. https://doi.org/10.5194/hess-19-4345-2015

Schwatke, C., Scherer, D., & Dettmering, D. (2019). Automated Extraction of Consistent Time-Variable Water Surfaces of Lakes and Reservoirs Based on Landsat and Sentinel-2. *Remote Sensing*, *11*(9), 1010. https://doi.org/10.3390/rs11091010

Schwatke, C., Dettmering, D., & Seitz, F. (2020). Volume Variations of Small Inland Water Bodies from a Combination of Satellite Altimetry and Optical Imagery. *Remote Sensing*, *12*(10), 1606. https://doi.org/10.3390/rs12101606

Shrivakshan, G. T. (2012). *A Comparison of various Edge Detection Techniques used in Image Processing* . *9*(5), 8.

Strahler, A. N. (1952). HYPSOMETRIC (AREA-ALTITUDE) ANALYSIS OF EROSIONAL TOPOGRAPHY. *Geological Society of America Bulletin*, *63*(11), 1117. https://doi.org/10.1130/0016-7606(1952)63[1117:HAAOET]2.0.CO;2

Tucker, C. J. (1979). *Red and Photographic Infrared l,lnear Combinations for Monitoring Vegetation*.

Vanthof, V., & Kelly, R. (2019). Water storage estimation in ungauged small reservoirs with the TanDEM-X DEM and multi-source satellite observations. *Remote Sensing of Environment*, *235*, 111437. https://doi.org/10.1016/j.rse.2019.111437

Wang, X., Xie, S., Zhang, X., Chen, C., Guo, H., Du, J., & Duan, Z. (2018). A robust Multi-Band Water Index (MBWI) for automated extraction of surface water from Landsat 8 OLI imagery. *International Journal of Applied Earth Observation and Geoinformation*, *68*, 73-91.

https://doi.org/10.1016/j.jag.2018.01.018
Willgoose, G., & Hancock, G. (1998). Revisiting the hypsometric curve as an indicator of form and process in transport-limited catchment. *Earth Surface Processes and Landforms*, *23*(7), 611-623.
Winslow, L.A., Read, J.S., Hanson, P.C. and Stanley, E.H. (2014), Lake shoreline in the contiguous United States: quantity, distribution and sensitivity to observation resolution. Freshw Biol, 59: 213-223. https://doi.org/10.1111/fwb.12258
Xu, H. (2006). Modification of normalised difference water index (NDWI) to enhance open water features in remotely sensed imagery. *International Journal of Remote Sensing*, *27*(14), 3025-3033. https://doi.org/10.1080/01431160600589179
Yang, J., & Du, X. (2017). An enhanced water index in extracting water bodies from Landsat TM imagery. *Annals of GIS*, *23*(3), 141-148. https://doi.org/10.1080/19475683.2017.1340339
Zhang, L., Liang, S., Yang, X., & Gan, W. (2020). Landscape evolution of the Eastern Himalayan Syntaxis based on basin hypsometry and modern crustal deformation. *Geomorphology*, *355*, 107085. https://doi.org/10.1016/j.geomorph.2020.107085
Zhang, S., Foerster, S., Medeiros, P., de Araújo, J. C., Duan, Z., Bronstert, A., & Waske, B. (2021). Mapping regional surface water volume variation in reservoirs in northeastern Brazil during 2009–2017 using high-resolution satellite images. *Science of The Total Environment*, *789*, 147711. https://doi.org/10.1016/j.scitotenv.2021.147711

Appendix B - GSW methodology to retrieve water extent

Using more than 30 years of 30m Landsat data, the JRC proposes the Global Surface Water (GSW) dataset (Pekel et al. 2016). The entire archive of the Landsat 5 Thematic Mapper (TM), the Landsat 7 Enhanced Thematic Mapper-plus (ETM+) and the Landsat 8 Operational Land Imager (OLI) orthorectified, top-of-atmosphere reflectance and brightness temperature images (L1T)31 acquired between 16 March 1984 and 10 October 2015 was used. Since 2016, they regularly produce monthly dataset from 1984 until now.

Techniques for big data exploration and information extraction less commonly used by the remote sensing community were exploited, namely expert systems, visual analytics, and evidential reasoning. Expert systems provide flexibility (to deal with the range of conditions encountered). Visual analytics combine human cognitive and perceptual abilities with the storage and processing capacities of cloud computing platforms. Evidential reasoning deals with problems related to both uncertainties and quality issues in the data set. Expert systems are non-parametric classifiers that can account for uncertainty in data, incorporate image interpretation expertise into the classification process, and can be used with multiple data sources. The expert system was developed to assign each pixel to one of three target classes, either water, land or non-valid observations (snow, ice, cloud or sensor-related issues). The inference engine of the system was a procedural sequential decision tree, which used both the multispectral and multitemporal attributes of the Landsat archive as well as ancillary data layers. Within the inference engine, expert knowledge was represented in the form of rules having the form: IF condition THEN inference. The condition contains equations describing the cluster hulls in a defined multispectral feature-space and can also be a combination of logical statements in which several components are linked through logical operators. The chaining of IF–THEN rules forms the problem-solving model that organizes and controls the steps and data used in the classification (see Figure 17). Tracing the line of reasoning used by the inference engine during the development phase meant that the reason for the class choice associated with each pixel could be retrieved, which in turn allowed the reasons behind classification challenges to be identified. Solutions to identified failings could then be developed using evidential reasoning and addressed in subsequent iterations so that the overall performance of the classifier was progressively improved. When the performance of the expert system could no longer be noticeably improved, it was applied to the entire Landsat L1T data set in a single run, and the output of this classification was then validated.

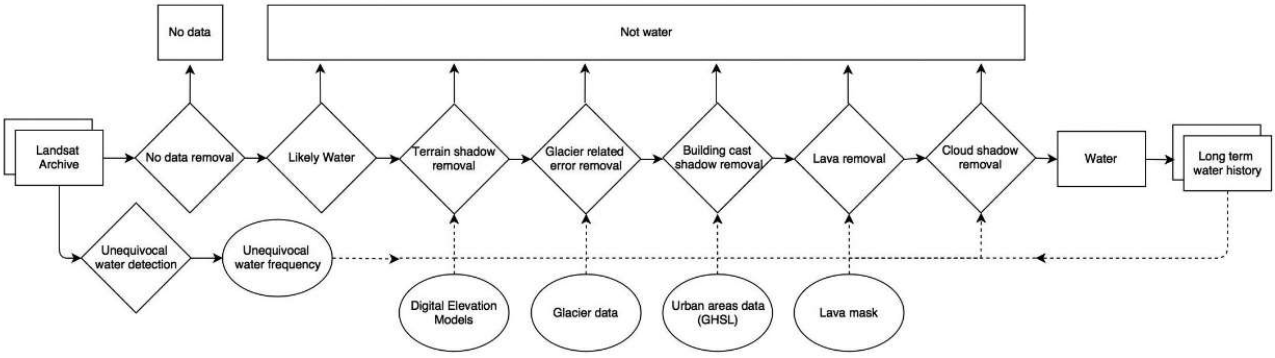

Figure 17 – Diagram of the expert system classifier (from Pekel et al., 2016)

The equations describing the cluster hulls used in the expert system were established through visual analytics. The first step was to build a spectral library capturing the spectral behavior of the three target classes across as wide a range of conditions as possible. 64,254 samples obtained through visual interpretation of 9,149 Landsat scenes recorded spectral variability of the target classes. Records held

in the library comprised spectral values from all bands. These records were enriched by deriving the Normalized Difference Vegetation Index and HueSaturation –Value (HSV) colour-space transformations for the following band combinations: shortwave infrared (SWIR2); near-infrared (NIR); red; and NIR/ green/blue using a standard transformation. The HSV colour model is well adapted for image analysis because the chromaticity (H and S) and the overall brightness (V) components are decoupled. This is highly desirable because changes in observation conditions first affect the V component and then the S component, while H remains relatively stable (except when the fundamental nature of the target changes, such as when land becomes water). Consequently, this property promotes temporal stability in the measurements and HSV-based classifications have been successfully used for near-real-time surface water detection at continental scales.

Ultimately, six products are proposed:

- Water occurrence
- Water occurrences change intensity
- Water seasonality
- Water recurrence
- Water transitions
- Water maximum water extent

Along with these six static products, monthly water body datasets are produced and retrievable at a nearly global scale, covering the 1984-2021 timespan (as of November 2022). They can be accessed through https://global-surface-water.appspot.com/download.

Now considered as unavoidable, the GSW dataset is nowadays used in numerous studies related to hydrology in general, and LSC estimation in particular (for instance Armon et al., 2020; Li et al. 2020;2021; Cooley et al., 2021; Hou et al., 2022).

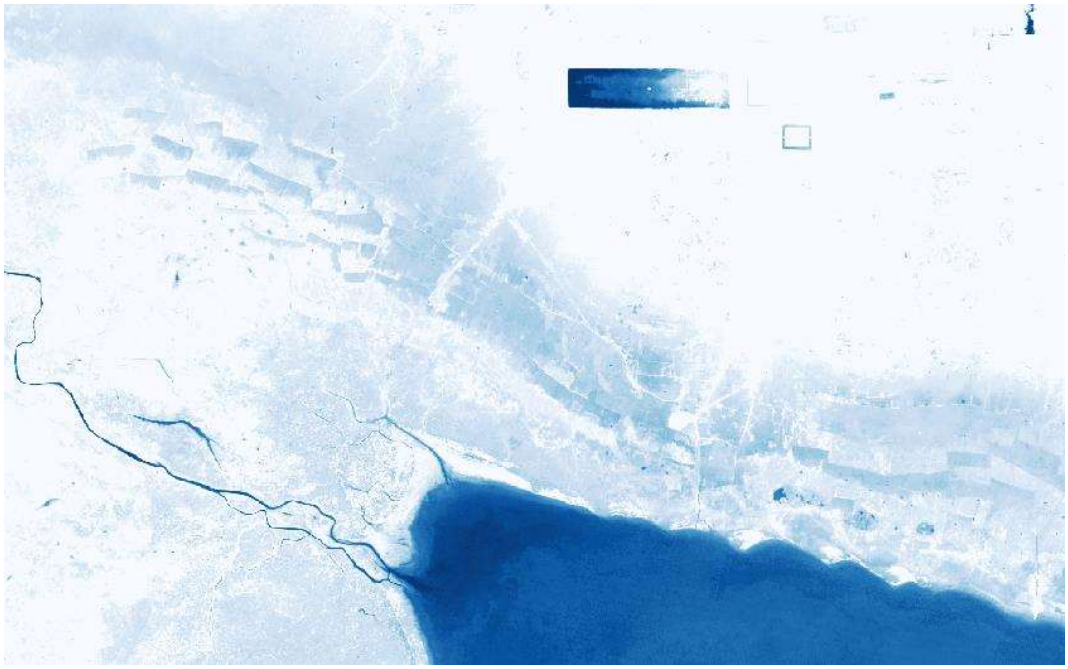

Figure 18 – Example of water occurrence from the GSW Occurrence dataset, here in Cambodia.